in CNM patients, at least in Japanese patients, further highlighting the importance of the frequency of ocular involvement as a genetic factor.

Other symptoms of the central nervous system and peripheral neuropathy were also observed in our cohort and were reported as subtle complications of DNM2-CNM [17]. Among the non-DNM2-CNM patients, other causative genes for CNM were considered. *MTM1* mutations are implicated in CNM, but in our cohort, *MTM1* mutations were excluded. Compound heterozygous mutations in *hJUMPY*, a gene that encodes a phosphoinositide phosphatase, were reported as a cause of sporadic CNM [8]. Additionally, *BIN1* is a newly identified causative gene for autosomal recessive CNM [9]; patients with autosomal recessive CNM show typical CNM muscle pathology and proximal-dominant muscle weakness, which is more severe than observed in DNM2-CNM patients. The pathology of CNM with *BIN1* mutations does not have a radial distribution, which is thought to be a hallmark of DNM2-CNM [9]. Notably, some of our non-DNM2-CNM patients showed a radial distribution. However, none of our non-DNM2-CNM patients had a family history that would indicate autosomal recessive inheritance and merit further mutational analysis of the *hJUMPY* and *BIN1* genes. Other candidate genes include *Srpk3* [20] and *PTPLA* [21], which were thus far implicated as causative genes of CNM in mice and dogs.

DNM2 mutations were also identified in AD Charcot–Marie–Tooth disease (CMT) [22]; in fact, some DNM2-CNM patients also show very mild reductions in nerve conduction velocities in the lower legs [10] or pathological changes in both myelinated and unmyelinated nerve fibers [18]. Nevertheless, none of our patients showed any abnormality in nerve conduction studies, suggesting that peripheral nerve involvement does not occur frequently in DNM2-CNM patients.

Although the precise pathomechanism of DNM2-CNM is not known, mutations are thought to hinder either the transport of DNM2 to the centrosome or its interaction with some centrosomal component [7]. Interestingly, in our study and past reports of *DNM2* mutations in the middle domain, characteristic features were observed in muscle pathology, as opposed to neonatal DNM2-CNM with PH domain mutations in which centrally nucleated fibers and radial distribution of myofibers are less prominent [11].

Acknowledgements

This work was supported in part by Research on Intractable Diseases of Health and Labour Sciences Research Grants, Comprehensive Research on Disability Health and Welfare, Health and Labour Science Research Grants, Intramural Research Grant (23-5 23-4) for Neurological and Psychiatric Disorders of NCNP and Young Investigator Fellowship from Translational Medical Center, National Center of Neurology and Psychiatry.

Appendix A. Supplementary data

Supplementary data associated with this article can be found, in the online version, at doi:10.1016/j.clineuro.2011.10.040.

References

[1] North K. In: Engel AG, Franzini-Armstrong C, Myology, editors. Congenital myopathies. 3rd ed. New York: McGraw-Hill; 2004. p. 1494–5.
[2] Jeannet PY, Mittaz L, Dunand M, Laforêt P, Urtizberea JA, Rouche A, et al. Clinical and histologic findings in autosomal centronuclear myopathy. Neurology 2004;11:1484–90.
[3] Wallgren-Petterson C, Clarke A, Samson F, Fardeau M, Dubowitz V, Moser H, et al. The myotubular myopathies: differential diagnosis of the X linked recessive, autosomal dominant, and autosomal recessive forms and present state of DNA studies. J Med Genet 1995;32:673–9.
[4] Sakuma T, Nakajima H, Fujimura C, Kimura F, Hanabusa T. A case of centronuclear myopathy with Charcot–Marie–Tooth disease-like lower leg muscle atrophy. Naika 2004;54:192–4 [in Japanese].
[5] Wakabayashi Y, Arimura Y, Sawaguchi Y, Koike F, Yoshino K. A case of myotubular myopathy with autosomal dominant inheritance. No to Shinkei 1980;32:715–22 [in Japanese].
[6] Bitoun M, Bevilacqua JA, Eymard B, Prudhon B, Fardeau M, Guicheney P, et al. A new centronuclear myopathy phenotype due to a novel dynamin 2 mutation. Neurology 2009;6:93–5.
[7] Bitoun M, Maugenre S, Jeannet PY, Lacène E, Ferrer X, Laforêt P, et al. Mutations in dynamin 2 cause dominant centronuclear myopathy. Nat Genet 2005;37:1207–9.
[8] Tosch V, Rohde HM, Tronchère H, Zanoteli E, Monroy N, Kretz C, et al. A novel PtdIns3P and PtdIns (3,5) P_2 phosphatase with an inactivating variant in centronuclear myopathy. Hum Mol Genet 2006;1:3098–106.
[9] Nicot AS, Toussaint A, Tosch V, Zanoteli E, Monroy N, Kretz C, et al. Mutations in *amphiphysin 2* (*BIN1*) disrupt interaction with dynamin 2 and cause autosomal recessive centronuclear myopathy. Nat Genet 2007;39:1134–9.
[10] Fischer D, Herasse M, Bitoun M, Barragán-Campos HM, Chiras J, Laforêt P, et al. Characterization of the muscle involvement in dynamin 2-related centronuclear myopathy. Brain 2006;129:1463–9.
[11] Bitoun M, Bevilacqua JA, Prudhon B, Barragán-Campos HM, Chiras J, Laforêt P, et al. Dynamin 2 mutations cause sporadic centronuclear myopathy with neonatal onset. Ann Neurol 2007;6:666–70.
[12] Jones SM, Howell KE, Henley JR, Cao H, McNiven MA. Role of dynamin in the formation of transport vesicles from the trans-Golgi network. Science 1998;23:573–7.
[13] Schafer DA, Weed SA, Binns D, Karginov AV, Parsons JT, Cooper JA. Dynamin2 and cortactin regulate actin assembly and filament organization. Curr Biol 2002;29:1852–7.
[14] Thompson HM, Cao H, Chen J, Euteneuer U, McNiven MA. Dynamin 2 binds gamma-tubulin and participates in centrosome cohesion. Nat Cell Biol 2004;6:335–42.
[15] Schessl J, Medne L, Hu Y, Zou Y, Brown MJ, Huse JT, et al. MRI in *DNM2*-related centronuclear myopathy: evidence for highly selective muscle involvement. Neuromuscul Disord 2007;17:28–32.
[16] Jeub M, Bitoun M, Guicheney P, Kappes-Horn K, Strach K, Druschky KF, et al. Dynamin 2-related centronuclear myopathy: clinical, histological and genetic aspects of further patients and review of the literature. Clin Neuropathol 2008;27:430–8.
[17] Echaniz-Laguna A, Nicot AS, Carré S, Franques J, Tranchant C, Dondaine N, et al. Subtle central and peripheral nervous system abnormalities in a family with centronuclear myopathy and a novel dynamin 2 gene mutation. Neuromuscul Disord 2007;17:955–9.
[18] Susman RD, Quijano-Roy S, Yang N, Webster R, Clarke NF, Dowling J, et al. Expanding the clinical, pathological and MRI phenotype of *DNM2*-related centronuclear myopathy. Neuromuscul Disord 2010;20:229–37.
[19] Liu D, Hsu WM. Oriental eyelids. Anatomic difference and surgical consideration. Ophthal Plast Reconstr Surg 1986;2:59–64.
[20] Nakagawa O, Arnold M, Nakagawa M, Hamada H, Shelton JM, Kusano H, et al. Centronuclear myopathy in mice lacking a novel muscle-specific protein kinase transcriptionally regulated by MEF2. Genes Dev 2005;19:2066–77.
[21] Pele M, Tiret L, Kessler JL, Blot S, Panthier JJ. SINE exonic insertion in the PTPLA gene leads to multiple splicing defects and segregates with the autosomal recessive centronuclear myopathy in dogs. Hum Mol Genet 2005;1:1417–27.
[22] Züchner S, Noureddine M, Kennerson M, Verhoeven K, Claeys K, De Jonghe P, et al. Mutations in the pleckstrin homology domain of dynamin 2 cause dominant intermediate Charcot-Marie-Tooth disease. Nat Genet 2005;37:289–94.

Available online at www.sciencedirect.com

SciVerse ScienceDirect

American Journal of OTOLARYNGOLOGY

ELSEVIER

American Journal of Otolaryngology–Head and Neck Medicine and Surgery 33 (2012) 758–761

www.elsevier.com/locate/amjoto

Case reports

Videofluorographic detection of anti–muscle-specific kinase–positive myasthenia gravis

Toshiyuki Yamamoto, MD, PhD*, Norio Chihara, MD, Madoka Mori-Yoshimura, MD, PhD, Miho Murata, MD, PhD

Department of Neurology, National Center Hospital of Neurology and Psychiatry, Tokyo, Japan

Received 19 March 2012

Abstract A 47-year-old woman with dysphagia and ptosis gradually developed dysarthria and muscular weakness. Magnetic resonance imaging, testing for anti–acetylcholine receptor antibodies, edrophonium chloride (EC) test, and electrophysiologic test revealed no abnormalities. A psychogenic reaction was suspected. Four months after disease onset, the patient presented to our hospital. In videofluoroscopic examination of swallowing (VF), there was no aspiration for swallowing of either liquid or soft food. It revealed, however, poor pharyngeal constriction, no epiglottis inversion, repeated swallowing movements, and large amounts of pharyngeal residue. Videofluoroscopic examination of swallowing after an intravenous injection of 10 mg EC showed improvements in all above observations; particularly, it was clear when swallowing soft food. Furthermore, the anti–muscle-specific kinase (MuSK) antibody titer was elevated, and anti-MuSK antibody–positive myasthenia gravis (MuSK-MG) was diagnosed. Thus VF during EC test may be helpful in diagnosing MuSK-MG in patients with dysphagia.

1. Introduction

Myasthenia gravis (MG) that is positive for anti–muscle-specific kinase (MuSK) (MuSK-MG) accounts for only 27% to 38% of anti–acetylcholine receptor (AChR) antibody–negative MG. Muscle-specific kinase MG is associated with bulbar symptoms, such as dysphagia and dysarthria, from an early stage [1-3]; therefore, these patients often present with the chief complaint of difficulty in swallowing. They need to consult an otolaryngologist before a definite diagnosis of MuSK-MG is made because MuSK antibody titer is measured in only some laboratories. The edrophonium chloride (EC) test, which evaluates the improvement of muscle weakness after intravenous EC injection, is positive in only 65.6% of patients with MuSK-MG in contrast to 88.6% of patients with anti–AChR antibody–positive MG (AChR-MG) [1,4].

Videofluoroscopic examination of swallowing (VF) before and after intravenous EC injection is useful for the evaluation of dysphagia during the course of AChR-MG [5,6]; however, whether it contributes to the diagnosis of MuSK-MG is unknown. This is the first case report that describes changes in swallowing movements before and after EC injection in a patient with MusK-MG.

2. Case report

A 47-year-old woman with dysphagia, dysarthria, ptosis, and general muscular weakness gradually developed difficulty in speaking and bilateral ptosis 1 month after the onset of difficulty in swallowing. Her medical, lifestyle, and family history were unremarkable.

The findings for cranial magnetic resonance imaging (MRI), neck MRI, and laboratory investigations were normal. The EC test was negative, and the cause of her symptoms

* Corresponding author. Department of Neurology, National Center Hospital of Neurology and Psychiatry, 4-1-1 Ogawahigashi-cho, Kodaira City, Tokyo 187-8551, Japan. Tel.: +81 42 341 2711; fax: +81 42 346 1705.
E-mail address: yamamoto@ncnp.go.jp (T. Yamamoto).

0196-0709/$ – see front matter © 2012 Elsevier Inc. All rights reserved.
http://dx.doi.org/10.1016/j.amjoto.2012.04.003

remained undiagnosed. At 2 months after symptom onset, the patient experienced choking while drinking water, could raise both arms only to the shoulder level, and had to hold on to railings when climbing stairs. After 3 months, she developed drooping of the neck (muscle weakness). The repetitive nerve stimulation test gave normal results, and the anti-AChR antibody test was negative; therefore, a psychogenic reaction was suspected. After 4 months, she presented to our hospital for the evaluation of dysphagia.

Blood pressure was 108/76 mm Hg, and the pulse was 86 per minute and regular. There was no respiratory distress, and the SpO_2 was 99%. Consciousness was intact. The patient complained of difficulty in chewing and swallowing food. Bilateral ptosis was observed. Hypernasality was noted with poor bilateral soft palate elevation. Facial muscle strength was decreased, and cheek puffing could not be maintained. Tongue protrusion was in the midline, and there was no atrophy or muscular fasciculation of the tongue. The gag reflex was intact. The proximal muscle groups were weaker than the distal muscle groups, with no left-right difference. No diurnal variations in muscle strength were observed. Tendon reflexes were decreased, and no pathologic reflexes were noted. Autonomic nervous symptoms, sensory disturbances, and cerebellar ataxia were not noted. Laboratory investigations, including thyroid function and creatine kinase levels, were normal. Respiratory functions and electrocardiogram were also normal.

We performed all x-ray fluoroscopic examinations after obtaining the patient's written informed consent, and the x-ray fluoroscopy time was less than 5 minutes. We evaluated the swallowing motion using 10 mL of 2-fold diluted 110% wt/vol barium solution (liquid) and 8 g of barium corned beef (soft food). The same evaluation was repeated after intravenous injection of 10 mg EC. All swallowing motions were recorded on DVD at 30 frames per second, and after the test, 1 examiner analyzed all VF clips using PC software Move-tr/2D 7.0 (Library Inc., Tokyo, Japan) and Adobe Photoshop CS5 (Adobe Systems Ins., San Jose, CA, USA).

The pharyngeal area before the start of swallowing (PA hold) [7] was 13.4 cm^2. On VF before EC injection, the liquid in the oral cavity could not be retained by the tongue and soft palate. Pharyngeal constriction during swallowing was poor, and the maximum pharyngeal constriction (PA max) [7] was 5.1 cm^2 with a pharyngeal constriction ratio (PCR) [7] of 0.38 (normal, 0.03 ± 0.03) [8]. The soft palate did not elevate, and the epiglottis did not invert (Fig, A). Liquid reflux into the mouth was noted. There was no aspiration for either liquid or soft food swallowing. After swallowing, both the liquid and the soft food remained in the epiglottic vallecula and piriform sinus. In particular, soft food residues remained at the base of the tongue and posterior hypopharyngeal wall (Fig, B). The pharyngeal transit duration (PTD) [9] for the soft food was 8.06 seconds. The number of swallows for the liquid was 8, whereas that for the soft food was 10.

On VF after EC injection, oral retention of the liquid was possible, and pharyngeal constriction improved. The PA max was 3.2 cm^2, and the PCR was 0.23. The soft palate did not elevate, but the epiglottis did invert (Fig, C). The PTD of the soft food improved to 6.15 seconds. There was no aspiration of the liquid or the soft food. The number of swallows decreased to 4 for the liquid and soft food each, and pharyngeal residues also decreased (Fig, D; Table). The patient was aware of the improvement in swallowing function after EC injection while consuming the soft food.

The anti-MuSK antibody titer was 10.03 nmol/L (normal, ≤ 0.05 nmol/L), and this led to a definitive diagnosis. The patient underwent 6 sessions of plasma adsorption therapy, and therapy with prednisolone 30 mg/d and tacrolimus 3.0 mg/d was initiated. The VF during treatment demonstrated that pharyngeal constriction was improved. When swallowing liquid, the number of swallows was 2; PA hold, 12.2 cm^2; PA max, 1.8 cm^2; and PCR, 0.15. When swallowing soft food, the number of swallows was 3; and PTD, 1.03 seconds. The pharyngeal residues of the liquid and the soft food decreased, but soft palate elevation remained moderately weak. The patient was aware of an improvement in swallowing function and was gradually able to eat normal diet. Muscle weakness and bilateral ptosis also improved, but mild hypernasality remained.

3. Discussion

In general, in swallowing liquids, there is a strong component of passive transport resulting from gravity, whereas active transport by tongue muscle retropulsion and pharyngeal muscle constriction has a greater role in swallowing soft foods [10]. In this patient, comparisons of the PA max and PCR before and after EC injection provided meaningful results in quantitative analysis. These improvements were due to temporary improvements in muscular strength with EC injection. For the soft food, the changes in PTD and improvement in pharyngeal retention were more obvious than for the liquid, suggesting abnormal active transport. Because of longer PTD, the change in swallowing soft food was more easily recognizable. The patient's awareness of the improvement in swallowing function after EC injection was also more apparent for soft food as with liquids. Our findings thus suggest that VF examination for soft food after intravenous EC injection would aid in diagnosing MuSK-MG even in the absence of abnormalities on electrophysiologic and laboratory tests.

In 70% of MuSK-MG patients, low doses of anticholinesterase drugs are effective; however, in 8.8% of MuSK-MG patients, a cholinergic crisis occurs despite these medications [11]. When performing VF after EC injection in MuSK-MG patients taking an anticholinesterase drug, the swallowing function may transiently worsen. Videofluoroscopic examination of swallowing during the EC test may be useful for differentiating MuSK-MG from other diseases that cause a bulbar syndrome; however, further studies are needed for evaluating the safety of this procedure.

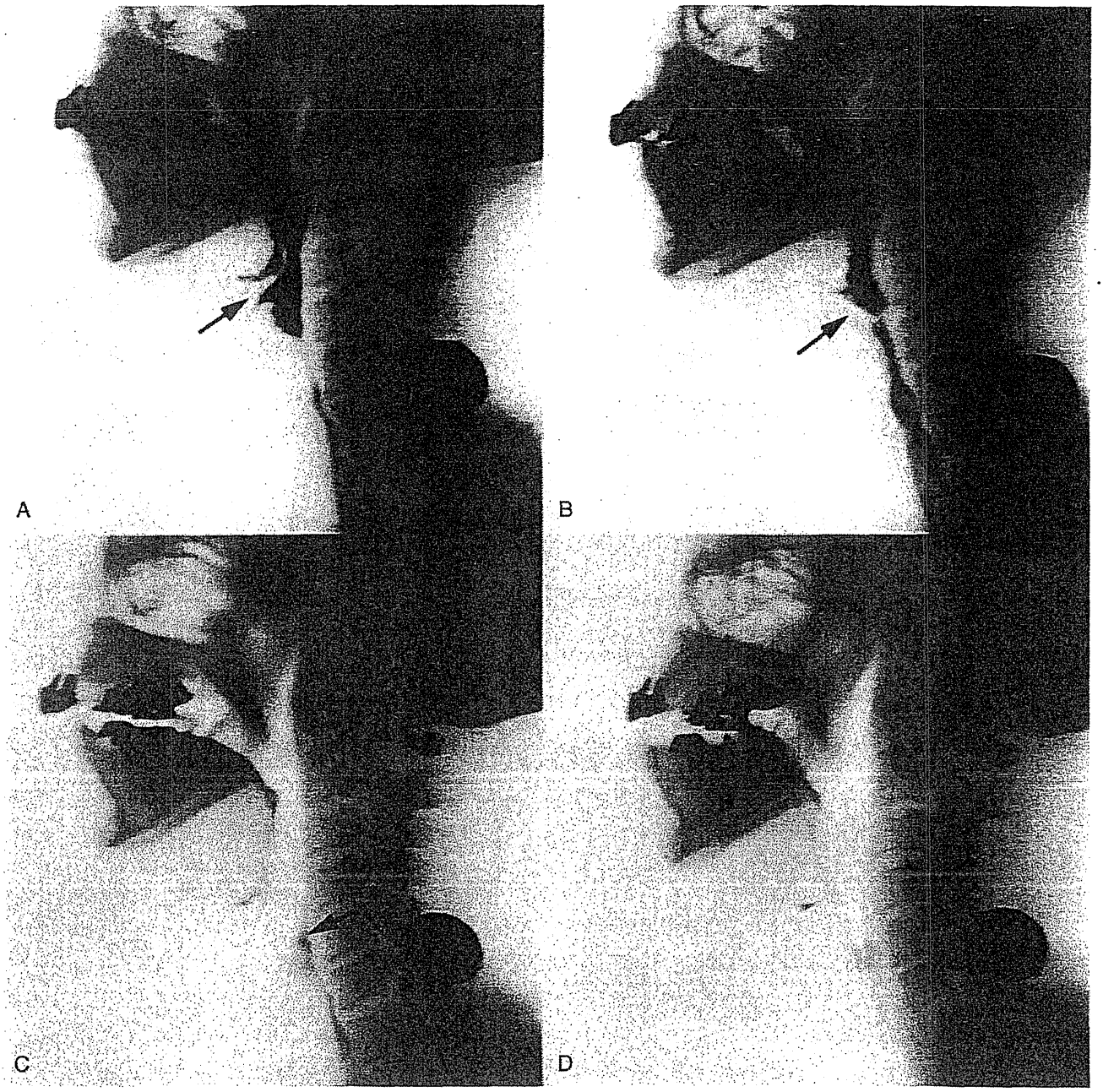

Fig. Videofluorography before and after intravenous injection of EC. A and C, Before EC injection. B and D, After EC injection. A and B, Maximum pharyngeal constriction during swallowing the liquid. C and D, Pharyngeal residue after swallowing the soft food. During swallowing the liquid before EC injection, the epiglottis did not invert at the point of maximum pharyngeal constriction (A, arrow), and pharyngeal constriction was insufficient, resulting in poor passage. After EC injection, although pharyngeal constriction was insufficient, the epiglottis inverted (B, arrow). When swallowing the soft food before intravenous EC, residue remained at the base of the tongue, epiglottic vallecula, piriform fossa, and posterior hypopharyngeal wall (C, arrow), whereas after EC injection, the pharyngeal residue was lesser (D). The circle in the figure is a marker for the maximum diameter of 23.5 mm.

This patient was originally suspected of having a psychogenic reaction before the swallowing function was evaluated. The diagnosis of psychogenic dysphagia should be made with caution and only after comprehensive evaluations [12]. Atrophy of the tongue muscles in early-stage MuSK-MG is often observed on MRI [13,14]. In this patient, atrophy from the tongue base to the pharynx was observed in the lateral view during x-ray fluoroscopy; this would be one of the useful findings to distinguish organic dysphagia from a psychogenic reaction, and it can be evaluated in a consulting room using an indirect laryngoscope. When patients with a chief complaint of dysphagia

Table
Comparison of videofluorography findings before and after EC injection

	Measurement parameter	Before EC injection	After EC injection
With liquid	PCR	0.38	0.23
	No. of swallows	8	4
	Soft palate elevation	None	None
	Epiglottis inversion	None	Present
	Pharyngeal residues	–	–
With soft food	No. of swallows	10	4
	PTD (s)	8.06	6.15
	Pharyngeal residues	–	–

have abnormal findings that suggest glossopharyngeal muscle weakness or atrophy, evaluation of swallowing after EC injection is advisable even if aspiration is not found in VF. This process might lead to a timely diagnosis of MuSK-MG, enabling the physician to take appropriate and timely therapeutic decisions.

4. Conflicts of interest

The authors declare that they have no conflicts of interest.

5. Ethics committee approval

All tests in this report were carried out in the normal course of medical treatment. Therefore, we did not apply for ethics committee approval.

6. Patient consent

Written informed consent regarding the submission of this article was obtained from the patient.

Acknowledgments

The authors thank Masakatsu Motomura of the First Department of Clinical Neuroscience and Neurology, Graduate School of Biomedical Sciences, Nagasaki University, Japan for measurement of the anti-MuSK antibody titers.

References

[1] Ohta K, Shigemoto K, Fujinami A, et al. Clinical and experimental features of MuSK antibody positive MG in Japan. Eur J Neurol 2007; 14:1029-34.
[2] Evoli A, Tonali PA, Padua L, et al. Clinical correlates with anti-MuSK antibodies in generalized seronegative myasthenia gravis. Brain 2003; 126:2304-11.
[3] Pasnoor M, Wolfe GI, Nations S, et al. Clinical findings in MuSK-antibody positive myasthenia gravis: a U.S. experience. Muscle Nerve 2010;41:370-4.
[4] Wolfe GI, Oh SJ. Clinical phenotype of muscle-specific tyrosine kinase-antibody–positive myasthenia gravis. Ann N Y Acad Sci 2008; 1132:71-5.
[5] Higo R, Nito T, Tayama N. Videofluoroscopic assessment of swallowing function in patients with myasthenia gravis. J Neurol Sci 2005;231:45-8.
[6] Schwartz DC, Waclawik AJ, Ringwala SN, et al. Clinical utility of videofluorography with concomitant Tensilon administration in the diagnosis of bulbar myasthenia gravis. Dig Dis Sci 2005;50:858-61.
[7] Leonard R, McKenzie S. Dynamic swallow study: instrumentation and measurement techniques. In: Leonard R, & Kendall K, editors. Dysphagia assessment and treatment planning: a team approach. San Diego, CA: Singular Publishing Group Inc.; 2008. p. 285-8.
[8] Leonard R, Rees CJ, Belafsky P, et al. Fluoroscopic surrogate for pharyngeal strength: the pharyngeal constriction ratio (PCR). Dysphagia 2009;26:13-7.
[9] Robbins JA, Logemann JA, Kirshner HS. Swallowing and speech production in Parkinson's disease. Ann Neurol 1986;19:283-7.
[10] Palmer JB. Bolus aggregation in the oropharynx does not depend on gravity. Arch Phys Med Rehabil 1998;79:691-6.
[11] Evoli A, Bianchi MR, Riso R, et al. Response to therapy in myasthenia gravis with anti-MuSK antibodies. Ann N Y Acad Sci 2008;1132: 76-83.
[12] Ravich WJ, Wilson RS, Jones B, et al. Psychogenic dysphagia and globus: reevaluation of 23 patients. Dysphagia 1989;4:35-8.
[13] Zouvelou V, Rentzos M, Toulas P, et al. MRI evidence of early muscle atrophy in MuSK positive myasthenia gravis. J Neuroimaging 2011; 21:303-5.
[14] Farrugia ME, Robson MD, Clover L, et al. MRI and clinical studies of facial and bulbar muscle involvement in MuSK antibody-associated myasthenia gravis. Brain 2006;129:1481-92.

$CCR2^+CCR5^+$ T Cells Produce Matrix Metalloproteinase-9 and Osteopontin in the Pathogenesis of Multiple Sclerosis

Wakiro Sato,*,[1] Atsuko Tomita,*,†,[1,2] Daijyu Ichikawa,* Youwei Lin,*,‡,§ Hitaru Kishida,† Sachiko Miyake,*,§ Masafumi Ogawa,‡,§ Tomoko Okamoto,‡,§ Miho Murata,‡ Yoshiyuki Kuroiwa,† Toshimasa Aranami,*,§ and Takashi Yamamura*,§

Multiple sclerosis (MS) is a demyelinating disease of the CNS that is presumably mediated by $CD4^+$ autoimmune T cells. Although both Th1 and Th17 cells have the potential to cause inflammatory CNS pathology in rodents, the identity of pathogenic T cells remains unclear in human MS. Given that each Th cell subset preferentially expresses specific chemokine receptors, we were interested to know whether T cells defined by a particular chemokine receptor profile play an active role in the pathogenesis of MS. In this article, we report that $CCR2^+CCR5^+$ T cells constitute a unique population selectively enriched in the cerebrospinal fluid of MS patients during relapse but not in patients with other neurologic diseases. After polyclonal stimulation, the $CCR2^+CCR5^+$ T cells exhibited a distinct ability to produce matrix metalloproteinase-9 and osteopontin, which are involved in the CNS pathology of MS. Furthermore, after TCR stimulation, the $CCR2^+CCR5^+$ T cells showed a higher invasive potential across an in vitro blood–brain barrier model compared with other T cells. Of note, the $CCR2^+CCR5^+$ T cells from MS patients in relapse are reactive to myelin basic protein, as assessed by production of IFN-γ. We also demonstrated that the $CCR6^-$, but not the $CCR6^+$, population within $CCR2^+CCR5^+$ T cells was highly enriched in the cerebrospinal fluid during MS relapse ($p < 0.0005$) and expressed higher levels of IFN-γ and matrix metalloproteinase-9. Taken together, we propose that autoimmune $CCR2^+CCR5^+$ $CCR6^-$ Th1 cells play a crucial role in the pathogenesis of MS. *The Journal of Immunology*, **2012, 189: 5057–5065.**

Multiple sclerosis (MS) is an inflammatory demyelinating disease of the CNS that is presumably mediated by $CD4^+$ T cells reactive to myelin Ag, such as myelin basic protein (MBP) (1). Approximately two thirds of patients with MS have relapsing-remitting MS (RR-MS), which is characterized by acute episodes of exacerbations followed by partial or complete recovery. Although there are periods of remission in the RR-MS stage, a proportion of patients enters a stage of secondary progressive MS decades after the onset of MS. There are no real periods of remission in secondary progressive MS, in which neurodegeneration can be the major cause of irreversible neurologic disability (2).

It is proposed that an initiation of relapse in RR-MS is preceded by activation of autoimmune $CD4^+$ T cells in the peripheral lymphoid organs. These T cells that are potentially reactive to myelin Ag could be activated in response to cross-reactive Ag that are generated by microbial infections (3) or following exposure to proinflammatory factors, such as osteopontin (OPN) (4), thereby acquiring the ability to migrate and infiltrate into the CNS (5, 6). The study performed in experimental autoimmune encephalomyelitis (EAE) showed that activated MBP-specific T cells first reach subarachnoid spaces filled with the cerebrospinal fluid (CSF) after crossing the endothelial barrier. After encountering perivascular APC presenting myelin Ag, the autoimmune T cells are reactivated and produce proinflammatory cytokines, such as IFN-γ and IL-17, as well as proteases, including matrix metalloproteinase (MMP)-9 (7). The proteases degrade components of the basement membranes, leading to the disruption of the blood–brain barrier (BBB). The T cells may invade into the parenchyma through the disrupted area of the BBB and cause CNS inflammation (8).

Research on EAE demonstrated that both IFN-γ–producing Th1 and IL-17–producing Th17 cells could cause inflammatory pathology in the CNS (9, 10). Although characterization of pathogenic T cells in EAE has ignited a search for similar cells in humans, the identity of pathogenic T cells in MS has not been established (10). Recent studies showed the involvement of Th17 cells (11) and of T cells producing both IFN-γ and IL-17 in the pathology of MS (12). However, because the administration of

*Department of Immunology, National Institute of Neuroscience, National Center of Neurology and Psychiatry, Tokyo 187-8502, Japan; †Department of Neurology and Stroke Medicine, Yokohama City University Graduate School of Medicine, Yokohama 236-0004, Japan; ‡Department of Neurology, National Center Hospital, National Center of Neurology and Psychiatry, Tokyo 187-8551, Japan; and §Multiple Sclerosis Center, National Center Hospital, National Center of Neurology and Psychiatry, Tokyo 187-8551, Japan

[1]W.S. and A.T. contributed equally to this work.

[2]Current address: Department of Neurology and Stroke Medicine, Yokohama City University Graduate School of Medicine, Yokohama, Japan.

Received for publication July 23, 2012. Accepted for publication September 11, 2012.

This work was supported by a Research Grant on Super Special Consortia for Supporting the Development of Cutting-Edge Medical Care from Cabinet Office, Government of Japan; a Grant-in-Aid for Scientific Research (S) from the Japan Society for the Promotion of Science (18189009 to T.Y.); and Research Grants on Psychiatric and Neurological Diseases and Mental Health and a Health and Labor Sciences Research Grant on Intractable Diseases (Neuroimmunological Diseases) from the Ministry of Health, Labor and Welfare of Japan.

Address correspondence and reprint requests to Dr. Takashi Yamamura and Dr. Toshimasa Aranami, Department of Immunology, National Institute of Neuroscience, National Center of Neurology and Psychiatry, 4-1-1 Ogawa-Higashi, Kodaira, Tokyo 187-8502, Japan. E-mail addresses: yamamura@ncnp.go.jp (T.Y.) and aranami@ncnp.go.jp (T.A.)

The online version of this article contains supplemental material.

Abbreviations used in this article: BBB, blood–brain barrier; CIS, clinically isolated syndrome; CSF, cerebrospinal fluid; EAE, experimental autoimmune encephalomyelitis; ECD, energy-coupled dye; HS, healthy subject; MBP, myelin basic protein; MMP, matrix metalloproteinase; MS, multiple sclerosis; NHA, normal human astrocyte; NIND, noninflammatory neurologic disease; OIND, other inflammatory neurologic disease; OPN, osteopontin; PB, peripheral blood; RR-MS, relapsing-remitting multiple sclerosis.

www.jimmunol.org/cgi/doi/10.4049/jimmunol.1202026

IFN-γ worsened MS in a previous clinical trial (13), the role of Th1 cells in MS needs to be analyzed further. In addition, increasing evidence suggest a pathogenic role for cytotoxic effector T cells in MS (14, 15). Moreover, a recent clinical trial of anti–IL-12p40 Ab to block IL-12/IL-23 signaling failed to modulate MS (16), making it difficult to portray a complete picture of MS (9).

Chemokines are a family of secreted proteins that function as key regulators of cell migration via interaction with a subset of seven-transmembrane, G protein-coupled receptors (17, 18). Chemokines are known to be highly efficient and potent chemoattractants for inflammatory cells in EAE (19). In the Th cell-differentiation process, $CD4^+$ T cells acquire the ability to produce sets of cytokines and to express chemokine receptors. Although Th1 cells preferentially express CCR5 and CXCR3, Th2 cells express CCR4 and CRTh2 (20, 21). The chemokine receptor expression pattern would confer to each Th subset a unique characteristic of migration to corresponding ligand chemokines (22). It was recently reported that human Th17 cells are enriched in $CCR4^+CCR6^+$, $CCR2^+CCR5^-$, and $CCR6^+$ populations (23–25).

The present study using multicolor flow cytometry was initiated to address whether Th17 cells bearing Th17 phenotypes ($CCR4^+$ $CCR6^+$, $CCR2^+CCR5^-$, or $CCR6^+$) are increased in the CSF of patients with MS compared with the peripheral blood (PB). In contrast to our expectations, none of these populations was increased in the CSF of MS. Instead, we found that T cells expressing both CCR2 and CCR5 were selectively enriched in the CSF of patients with exacerbated MS but not in patients with other neurologic diseases. The $CCR2^+CCR5^+$ memory $CD4^+$ T cells were shown to produce IFN-γ (24). Comparison with other memory T cell subpopulations revealed that the $CCR2^+CCR5^+$ T cells possessed a distinct ability to produce MMP-9 and OPN, which are critical for initiating and perpetuating the inflammatory pathology in the CNS (4, 7). Consistent with the increased production of MMP-9, which is capable of degrading basement membranes, the $CCR2^+$ $CCR5^+$ T cells showed a greater potential to invade across an in vitro model of the glia limitans, the physiological barrier separating CSF from the CNS parenchyma. Furthermore, the $CCR2^+CCR5^+$ T cells in the PB of active MS contained MBP-reactive T cells producing IFN-γ. We further demonstrated that $CCR6^-$, but not $CCR6^+$, cells within $CCR2^+CCR5^+$ T cells were enriched in the CSF of patients with MS during relapse and expressed high levels of IFN-γ and MMP-9. These results suggest that $CCR2^+CCR5^+CCR6^-$ Th1 cells play a crucial role in the pathogenesis of MS.

Materials and Methods

Subjects

Thirty-four RR-MS patients were examined for the expression of chemokine receptors on T cells. As controls for MS, 11 sex- and age-matched healthy subjects (HS), 6 patients with noninflammatory neurologic disease (NIND), and 4 patients with other inflammatory neurologic disease (OIND) were enrolled in this study. All of the MS patients fulfilled the diagnostic criteria of McDonald et al. (26). Patients with serum aquaporin 4 Abs or with longitudinally extensive spinal cord lesions on the magnetic resonance imaging scan were excluded from this study. In this article, we define "MS in remission" as patients who have been clinically stable without i.v. corticosteroid pulse therapy for >1 mo; "MS in relapse" is defined as patients who have developed an apparent exacerbation within an interval of 1 wk. The detailed demographic characteristics of the cohorts are summarized in Table I. None of the above patients had received IFN-β, i.v. corticosteroids, other immunomodulatory drugs, plasma exchange, or i.v. Ig for ≥1 mo before blood sampling.

CSF and PB pairs were obtained from 12 MS patients in relapse, 6 NIND patients, and 4 OIND patients (Table I). Although NIND patients were significantly older than the MS patient cohort, we confirmed that there was no correlation between age and the frequency of T cell subsets in the CSF of NIND patients. All MS patients were recruited from the National Center Hospital, National Center of Neurology and Psychiatry. OIND patients were recruited from the Yokohama City University Graduate School of Medicine. Written informed consent was obtained from all of the subjects. The National Center of Neurology and Psychiatry Ethics Committee approved this study.

Reagents

Anti–CCR2-biotin, anti–CCR5-FITC, anti–CCR6-FITC, and anti–CCR7-FITC mAb were purchased from R&D Systems (Minneapolis, MN). Streptavidin-PE, streptavidin–energy-coupled dye (ECD), anti–CD45RA-ECD, and mouse IgG1-FITC mAb were purchased from Beckman Coulter (Brea, CA). Anti–CD4-PerCP-Cy5.5, anti–CCR4-PE-Cy7, anti–CCR5-allophycocyanin, anti–CCR4-PE, and anti–CCR6-biotin mAb were purchased from BD Biosciences (San Jose, CA). Human MBP was prepared as described previously (27). For cell culture medium, we used RPMI 1640 (Invitrogen, La Jolla, CA) supplemented with 0.05 mM 2-ME, 2 mM L-glutamine, 100 U/ml penicillin/streptomycin, and 10% FBS.

Cell preparation

PBMC were freshly isolated by density-gradient centrifugation using Ficoll-Paque Plus (GE Healthcare, Oakville, ON, Canada). We used a Memory $CD4^+$ T cell isolation kit (Miltenyi Biotec, Bergisch Gladbach, Germany) to purify memory $CD4^+$ T cells from PBMC. Briefly, PBMC were labeled with a mixture of biotin-conjugated mAb directed against nonmemory $CD4^+$ T cells and then reacted with magnetic microbead-conjugated anti-biotin mAb. The magnetically labeled nonmemory $CD4^+$ T cells were depleted with auto-MACS (Miltenyi Biotec), which yielded >80% purity of memory $CD4^+$ T cells, as assessed by flow cytometry.

To further separate memory $CD4^+$ T cells according to CCR2, CCR5, CCR4, and CCR6 expression, the cells were labeled with anti–CCR2-biotin, anti–CCR5-allophycocyanin, anti–CCR4-PE-Cy7, and anti–CCR6-FITC mAb and streptavidin-PE, in addition to CD4-PerCP-Cy5.5 and CD45RA-ECD. The stained cells were separated by a flow cytometric cell sorter (FACSAria; BD Biosciences). To measure Ag-specific responses, memory $CD4^+$ T cells were separated into $CCR2^+CCR5^+$ T cells and those depleted of $CCR2^+CCR5^+$ T cells by the cell sorter FACSAria II (BD Biosciences). To prepare APC, PBMC depleted of memory $CD4^+$ T cells were stained with anti–CD3-allophycocyanin-Cy7 and anti–CD56-PE mAb. Subsequently, $CD3^-CD56^-$ cells were sorted by FACSAria II and used as APC. This procedure yielded >95% purity of the cells.

Flow cytometric analysis of chemokine receptors

To evaluate expression of chemokine receptors on memory $CD4^+$ T cells, PBMC were first labeled with magnetic microbead-conjugated anti-CD14 mAb, and the labeled $CD14^+$ cells were depleted with auto-MACS, which yielded >95% purity of non-$CD14^+$ PBMC. $CD14^+$ cell-depleted PBMC were stained with anti–CD4-PerCP-Cy5.5, anti–CD45RA-ECD, anti–CCR2-biotin, anti–CCR5-allophycocyanin, anti–CCR4-PE-Cy7, and anti–CCR6-FITC mAb, as well as streptavidin-PE. anti–CCR7-FITC, anti–CCR4-PE, and anti–CCR6-biotin mAb and streptavidin-ECD were used for the staining of CCR7. CSF cells were stained directly with the above-mentioned Abs without depleting $CD14^+$ cells. An isotype control of each Ab was used as a negative control. At the end of the incubation, cells were washed and resuspended in PBS supplemented with 0.5% BSA and immediately analyzed by FACSAria.

Cell culture and cytokine measurements by ELISA

Purified memory $CD4^+$ T cell subsets were suspended at 5×10^5 cells/ml and stimulated with PMA (50 ng/ml) and ionomycin (500 ng/ml) in 96-well U-bottom plates for 24 h. The concentrations of IFN-γ, IL-17, and OPN in the supernatants were measured by Human IFN-γ ELISA Set (BD Biosciences), Human IL-17 DuoSet (R&D Systems), and Human Osteopontin DuoSet (R&D Systems). The procedures were performed according to the manufacturers' instructions.

Intracellular cytokine staining of IL-17 and IFN-γ

Purified memory $CD4^+CCR2^+CCR5^+$ and $CD4^+CCR2^-CCR5^+$ T cells were stimulated with PMA and ionomycin in the presence of monensin for 18 h, fixed in PBS containing 2% paraformaldehyde, and permeabilized with 0.1% saponin. Subsequently, the cells were stained with anti–IL-17-Alexa Fluor 488 and anti–IFN-γ-PE-Cy7 mAb (eBioscience, San Diego, CA). Mouse IgG1-Alexa Fluor 488 and Mouse IgG1-PE-Cy7 were used as isotype control Abs.

T cell stimulation with MBP

To assess the presence of memory MBP-reactive T cells in the purified T cell subsets, FACS-sorted T cell subsets (2×10^4 cells/well) were cocultured

with the irradiated (3500 rad) APC (2×10^5 cells/well), in the presence or absence of MBP (10 μg/ml) or OVA (10 μg/ml), in 96-well flat-bottom plates for 5 d. rIL-2 (20 IU/ml) was added to support the growth of T cells. Cytokine concentrations in the culture supernatants were measured by ELISA.

Real-time RT-PCR

FACS-sorted cells were stimulated with PMA and ionomycin for 12 h, as described above. Total RNA was extracted from cultured cells with an RNeasy Mini Kit (QIAGEN, Tokyo, Japan), according to the manufacturer's instructions. cDNA was synthesized with a PrimeScript RT-PCR kit using oligo-dT Primers (Takara Bio, Otsu, Shiga, Japan). Gene expression was quantified by LightCycler (Roche Diagnostics, Indianapolis, IN) with SYBR Premix Ex Taq (Takara Bio). All procedures were performed according to the manufacturers' protocols. mRNA levels were normalized to endogenous β-actin (ACTB) in each sample. The specific primers used in this study are listed in Table III.

Zymography

MMP-9 activity was determined as previously reported (28). Briefly, SDS-polyacrylamide gels were copolymerized with 1 mg/ml type A gelatin derived from porcine skin (Sigma-Aldrich, St. Louis, MO). $CCR2^+CCR5^+$ T cells and $CD4^+$ T cells depleted of $CCR2^+CCR5^+$ T cells were stimulated with PMA and ionomycin, and 20 μl the culture supernatant and recombinant MMP-9 were electrophoresed. The gels were washed twice in 2% Triton X-100 for 30 min and incubated for 18 h at 37°C in buffer (150 mM NaCl, 50 mM Tris-HCl, 5 mM $CaCl_2$, and 0.02% NaN_3, [pH 7.5]). After fixing with methanol containing acetic acid, the gels were stained with 0.1% Coomassie blue R-250 (Nakarai Tesque, Kyoto, Japan). The gels were scanned with a UV transilluminator (BioDoc-It Imaging System, UVP, Upland, CA) in grayscale mode, and the image was inverted by Adobe Photoshop (Adobe Systems, Mountain View, CA). Recombinant MMP-9 (GE Healthcare) was used as a positive control.

Migration assay

Migration assays were performed with 24-well Transwell membrane inserts (Corning, Wilkes-Barre, PA). The upper sides of Transwell membrane inserts (8 μm; Corning) were coated with 10 μg/ml laminin-1 (Sigma) or 20 μg/ml laminin-2 (Bio Lamina, Stockholm, Sweden). After aspirating the laminin solutions, the membrane inserts were turned upside down, and normal human astrocytes (NHA; Takara Bio) were seeded on the lower sides of the membrane inserts (2×10^5/well). After 18 h, astrocytes formed a confluent monolayer, as confirmed by Diff-Quick staining. Then the membranes were washed twice with RPMI 1640 medium supplemented with 10% FBS and settled in a 24-well plate. PBMC from HS were sorted into memory $CD4^+CCR2^+CCR5^+$ T cells, memory $CD4^+$ T cells depleted of $CCR2^+CCR5^+$ T cells, and memory $CD4^+$ T cells by flow cytometry. These T cells were stimulated with plate-bound anti-CD3/CD28 mAb for 60 h. Then the cells were harvested, suspended in the fresh medium, and seeded onto the upper chambers at 1×10^5 cells/ well, and 600 μl the medium was added to the lower chambers. After 8 h, 500 μl cell suspension was collected from the lower chambers after careful pipetting, and absolute numbers of migrated cells were counted by flow cytometry using Trucount tubes (BD Bioscience).

Statistics

A one-way ANOVA test was used to compare the frequency of chemokine receptor expression within each group of patients or HS. A paired Student *t* test was used to evaluate the difference in the percentage inhibition of migration and in the frequency of chemokine receptor expression between PB and CSF from the same patients. For statistical analysis of other data, an unpaired Student *t* test or one-way ANOVA was used. The *p* values < 0.05 were considered statistically significant.

Results

$CCR2^+CCR5^+$ T cells are enriched in the CSF of MS patients in relapse

First, we analyzed the chemokine receptor-expression profile of memory $CD4^+$ T cells in the PB of MS patients (Table I) compared with HS and those with NIND. Multicolor flow cytometric analysis was performed on PBMC after staining with differentially labeled anti-CCR2, -CCR4, -CCR5, and -CCR6 mAb. Patterns of coexpression for four chemokine receptors are summarized in Supplemental Fig. 1 and Supplemental Table I. When the memory T cells in PB were grouped based on CCR2 versus CCR5 or CCR4 versus CCR6 expression (Fig. 1A), no particular population was found to be altered in MS patients compared with HS or NIND patients, irrespective of whether the MS patients were in relapse or in remission (Fig. 1B). We next analyzed sets of CSF and PB samples from individual patients with MS, OIND, or NIND. As shown in Fig. 1C, $CCR2^-CCR5^+$ T cells formed the predominant T cell population in the CSF of patients with NIND or MS during relapse, suggesting that this population, which was previously shown to be enriched for Th1 cells (24), is allowed to enter the CSF spaces in the patients with MS and NIND. It was reported that human IL-17–producing T cells or Th17 cells are enriched in $CCR2^+CCR5^-$, $CCR4^+CCR6^+$, or $CCR6^+$ cells (23–25). We were initially interested in knowing whether examination of the chemokine receptor profile could reveal an increase in Th17 cells in the CSF of MS patients. However, the frequencies of $CCR2^+CCR5^-$, $CCR4^+CCR6^+$, and $CCR6^+$ cells were lower, rather than higher, in the CSF compared with the PB of patients with MS or NIND. In contrast, the frequency of $CCR2^+CCR5^+$ T cells in the CSF of patients with MS was significantly higher than in the PB (Fig. 1C). Of note, this increase was specific for MS and was not found in the patients with other neurologic diseases, indicating that cells of this subset are selectively recruited to autoimmune inflammatory lesions or would expand in the CSF during relapse of MS. In addition, if we separate the MS patients by disease duration (<10 y [$n = 8$] or >10 y [$n = 4$]), the higher frequency of $CCR2^+CCR5^+$ T cells in CSF compared with PB was evident ($p < 0.0005$) in those with the shorter history of MS (<10 y) (Fig. 2, Table II), but not in those with longer history (data not shown). We also noted that enrichment for $CCR2^-CCR5^+$ T cells in the CSF was not detected in the patients with the shorter history of MS. In contrast, the proportion of $CCR4^+CCR6^+$ T cells was significantly lower ($p < 0.005$) in CSF compared with PB of these

Table I. Patient summary

PB Analysis	MS in Remission	MS in Relapse	HS	NIND[a]
Males/females (*n*)	3/8	5/6	5/6	2/4
Age (y; mean ± SD)	44 ± 12	42 ± 13	39 ± 5	64 ± 13
PB/CSF Analysis	**MS in Relapse[b]**	**NIND**	**OIND[c]**	
Males/females (*n*)	5/7	2/4	2/2	
Age (y; mean ± SD)	46 ± 15	64 ± 13	44 ± 14	

[a]NIND includes one patient with Parkinson's disease, one patients with myasthenia gravis, three patients with normal pressure hydrocephalus, and one patient with multiple system atrophy.

[b]Five MS patients were being treated with immunomodulatory drugs (one with IFN-β, two with oral corticosteroids, and two with an immunosuppressive drug) before their relapses.

[c]OIND includes one patient with mumps meningitis, one patient with herpes encephalitis, and two patients with undiagnosed viral meningitis in acute phase.

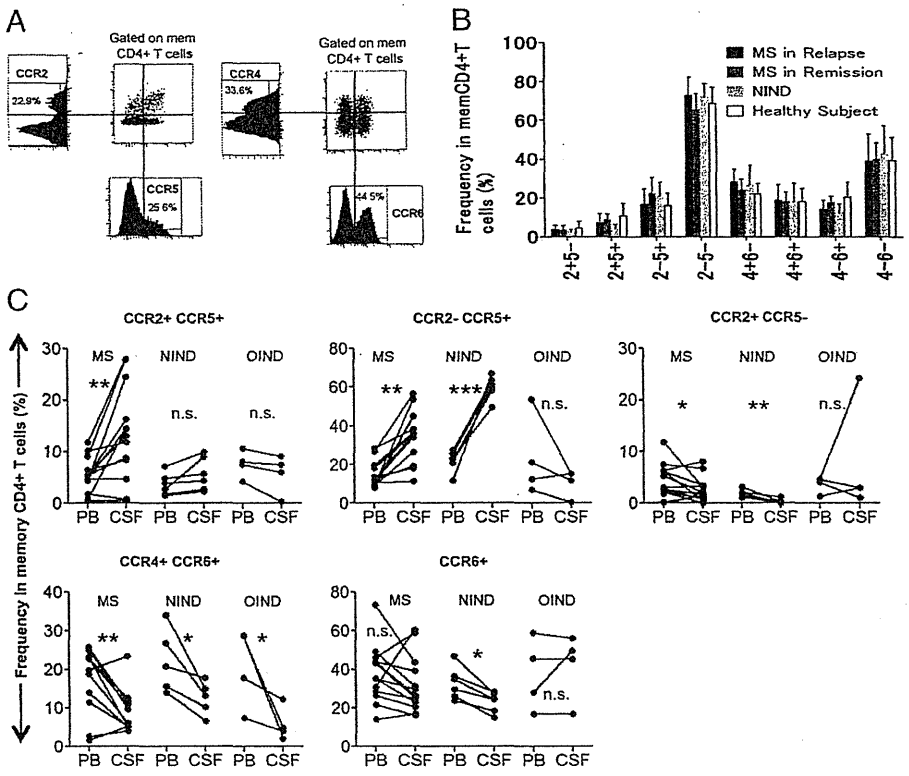

FIGURE 1. $CCR2^+CCR5^+$ T cells are enriched in the CSF of MS patients in relapse. **(A)** PBMC depleted of $CD14^+$ cells were stained with differentially labeled anti-CD4, -CD45RA, -CCR2, -CCR5, -CCR4, and -CCR6 mAb simultaneously. The $CD4^+CD45RA^-$ population was analyzed for expression of CCR2 and CCR5 (*left panels*) or CCR4 and CCR6 (*right panels*). Graphs of the corresponding parameters are also shown. Numbers (%) indicate the percentage of the positive population in the graphs. **(B)** Cells were stained, as described in (A), and frequencies of T cell subsets in memory $CD4^+$ T cells of 11 MS patients in relapse, 11 MS patients in remission, 6 NIND patients, and 11 HS were calculated. For brevity, "CCR" is omitted from the figure (e.g., 2+5− represents $CCR2^+CCR5^-$). **(C)** Comparison of the frequencies of the T cell subsets in the CSF and PB from 12 MS patients in relapse, 6 patients with NIND, and 4 patients with OIND. Lines connect data for paired CSF and PB samples from the same patients. $^*p < 0.05$, $^{**}p < 0.005$, $^{***}p < 0.0005$. n.s., Not significant.

MS patients. These results indicate that selective enrichment of $CCR2^+CCR5^+$ T cells in the CSF is detected in relatively early stages of MS.

$CCR2^+CCR5^+$ T cells in the PB contain both central and effector memory cells and produce both IFN-γ and IL-17

Memory $CD4^+$ T cells are divided into $CCR7^+$ central memory and $CCR7^-$ effector memory subsets, which are differentially endowed with effector functions (29). The staining of CCR7, together with CCR2/5 or CCR4/6, revealed a higher effector memory/central memory ratio in $CCR2^+CCR5^+$ T cells and $CCR2^-CCR5^+$ T cells (Supplemental Fig. 2). We next analyzed cytokine production by each T cell population bearing a distinct chemokine receptor profile. The cells of interest were separated from PB of HS and were stimulated with PMA and ionomycin. Compared with unfractionated memory $CD4^+$ T cells, $CCR2^+CCR5^+$ and $CCR2^-CCR5^+$ T cells produced a larger quantity of IFN-γ (Fig. 3A). Although $CCR2^+CCR5^+$ T cells produced a significant amount of IL-17, production of IL-17 from $CCR2^-CCR5^+$ T cells was only marginal. $CCR2^+CCR5^-$ T cells and $CCR4^+CCR6^+$ T cells selectively produced IL-17, whereas $CCR4^-CCR6^-$ T cells selectively produced IFN-γ. These results were consistent with the results of previous studies (23, 24). Because T cells expressing both IFN-γ and IL-17 are reportedly present in highly infiltrated lesions of MS brain sections (12), it was of interest to know whether similar T cells producing both IFN-γ and IL-17 are present in $CCR2^+$ $CCR5^+$ T cells. By conducting intracellular cytokine staining, we revealed that the $CCR2^+CCR5^+$ T cells, as well as $CCR2^-CCR5^+$ T cells, are composed of IFN-γ^+IL-17^- cells, IFN-γ^+IL-17^+ cells,

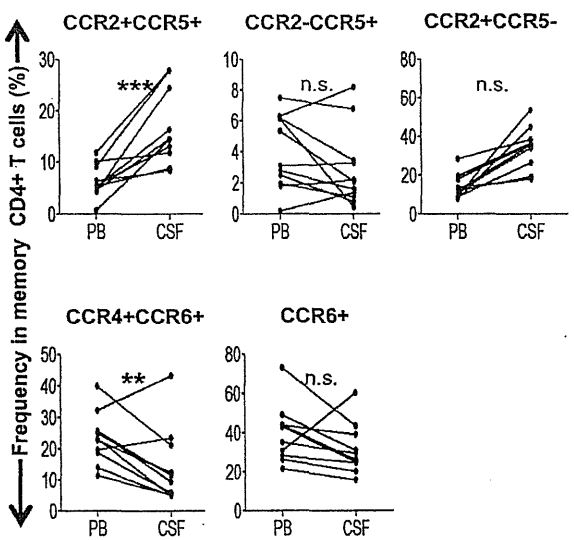

FIGURE 2. Frequencies of the T cell subsets in the CSF and PB from eight MS patients with disease duration <10 y. $^{**}p < 0.005$, $^{***}p < 0.0005$. n.s., Not significant.

Table II. $CCR2^+CCR5^+$ T cells are involved in early stages of MS

Clinical Parameter	Disease History <10 y	Disease History >10 y
Disease duration (y; mean ± SD)	4.8 ± 3.8	15.5 ± 4.4
No. of patients	8[a]	4[b]
Age (y; mean ± SD)	42 ± 14	54 ± 15
Relapse rate (times/y; mean ± SD)	1.8 ± 0.9	2.0 ± 14
EDSS (mean ± SD)	3.1 ± 0.7	4.0 ± 1.2
No. of patients with more $CCR2^+CCR5^+$ T cells in CSF than in PB	8*	0

[a]Three patients were treated with IFN-β ($n = 1$), oral steroid ($n = 1$), or immunosuppressant ($n = 1$).
[b]Two patients were treated with oral steroid.
$^*p < 0.0005$.

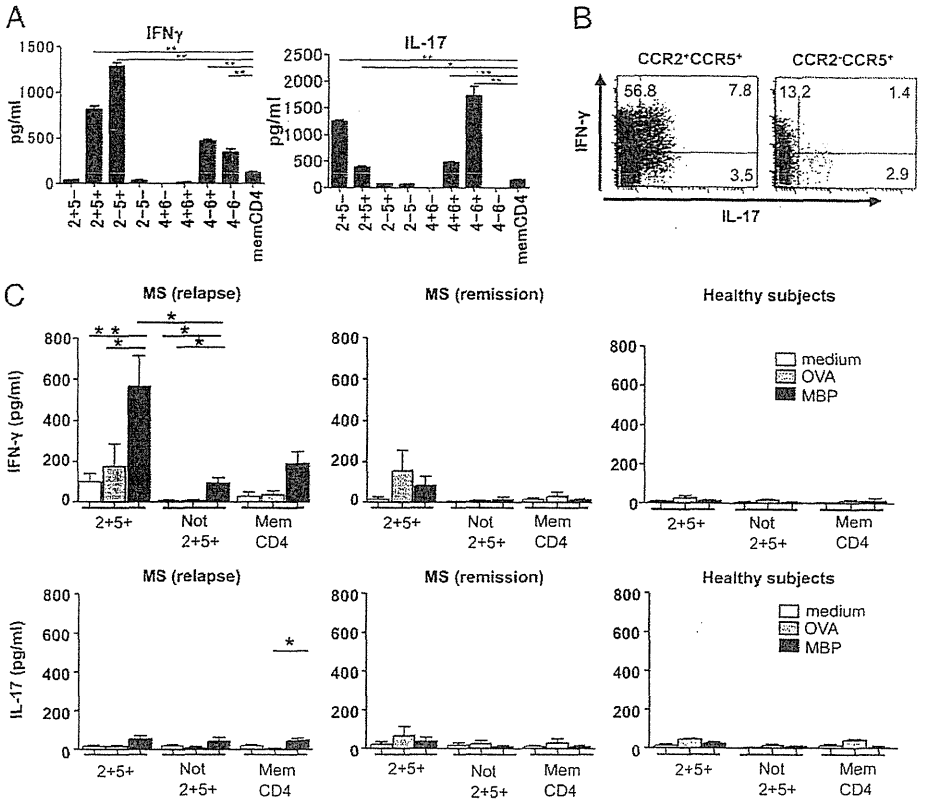

FIGURE 3. Cytokine production and reactivity to MBP by $CCR2^+CCR5^+$ T cells in the PB. (**A**) Memory $CD4^+$ T cell subsets purified from PBMC of HS by flow cytometry were stimulated with PMA and ionomycin. Concentrations of IFN-γ and IL-17 in the supernatants were measured by ELISA. Data represent mean ± SD of three HS. (**B**) Purified $CCR2^+CCR5^+$ T cells (*left panel*) and $CCR2^-CCR5^+$ T cells (*right panel*) were stimulated with PMA and ionomycin for 18 h, and the production of IL-17 and IFN-γ was assessed by intracellular cytokine staining. Numbers indicate the frequency (%) of cells in each quadrant. One representative experiment from three independent experiments with PBMC from HS is shown. (**C**) Purified memory $CD4^+$ T cell subsets were cultured in duplicate with irradiated APC in the presence of MBP (10 μg/ml) or OVA (100 μg/ml) for 5 d. Concentrations of IFN-γ and IL-17 in the supernatants were measured by ELISA. Data represent mean ± SD of six MS patients in relapse, three MS patients in remission, and three HS. $*p < 0.05$, $**p < 0.005$.

and IFN-γ^-IL-17^+ cells (Fig. 3B). In both T cell populations, IFN-γ^+IL-17^- cells were a major subset of IFN-γ production.

$CCR2^+CCR5^+$ T cells in the PB from MS patients during relapse are reactive to MBP

Given that the $CCR2^+CCR5^+$ T cells are proportionally higher in CSF than PB of MS during relapse, we were interested to know whether the $CCR2^+CCR5^+$ T cells are enriched in autoimmune, pathogenic T cells. We therefore examined if the $CCR2^+CCR5^+$ T cells might react to MBP, a putative autoantigen for MS. We isolated memory $CD4^+CCR2^+CCR5^+$ T cells and memory $CD4^+$ T cells depleted of $CCR2^+CCR5^+$ T cells from the PB of MS in relapse, MS in remission and HS. We stimulated these cells with MBP or OVA in the presence of autologous APC and measured the levels of IFN-γ and IL-17 in the supernatants after culture (Fig. 3C). The T cell populations separated from HS did not show any significant response to MBP or OVA in this assay. A marginal IFN-γ response to MBP and OVA was noted in $CCR2^+CCR5^+$ T cells from MS in remission. Strikingly, the $CCR2^+CCR5^+$ T cells from MS in relapse selectively and significantly responded to MBP by producing a large amount of IFN-γ, whereas those depleted of $CCR2^+CCR5^+$ T cells or total memory $CD4^+$ T cells showed a much smaller response. These results suggest that MBP-specific IFN-γ-producing cells might be enriched in $CCR2^+$ $CCR5^+$ T cells during relapse of MS.

$CCR2^+CCR5^+$ T cells in the PB produce MMP-9 and OPN

Lymphocyte migration/infiltration is a critical step for the development of autoimmune pathology in the CNS, and two physical barriers protect the CNS parenchyma from entry of the immune cells: the vascular endothelium barrier and the glia limitans barrier made up of extending astrocyte foot processes (8, 30). Each barrier possesses its own basement membrane, and the CSF circulates in the perivascular space between the two membranes. Thus, initiation of CNS inflammation requires immune cells that are capable of disrupting these physical barriers. Because type IV collagenase MMP-9 is selectively elevated in the CSF in MS, MMP-9 is assumed to play a role in disrupting the BBB in MS (28, 31, 32). Speculating that $CCR2^+CCR5^+$ T cells may have a distinct ability to initiate the processes of CNS inflammation, we examined whether $CCR2^+CCR5^+$ T cells are able to produce MMP-9. Strikingly, quantitative RT-PCR analysis of whole and CCR2/CCR5 fractions of memory T cells from HS and MS showed that expression of MMP-9 was mainly restricted to $CCR2^+CCR5^+$ T cells (Fig. 4A, 4B, Table III). The expression of MMP-1 and MMP-19, which also possess the potential to degrade the basement membrane, was highest in $CCR2^+CCR5^+$ T cells, whereas all T cell populations similarly expressed MMP-10 and MMP-28 (Supplemental Fig. 3). We also measured MMP-2, -7, -14, -15, -23, and -25, but none of these was detected. Using zymography, we further examined MMP-9 enzymatic activity in the culture supernatants of activated $CCR2^+CCR5^+$ T cells. As shown in Fig. 4C, supernatants from $CCR2^+CCR5^+$ T cells exhibited MMP-9 activity, but those from T cells depleted of the $CCR2^+CCR5^+$ population did not.

Recent studies suggested that OPN, which is also expressed by T cells (33, 34), might be involved in the pathogenesis of MS. Although OPN-deficient mice were resistant to relapse of EAE (4, 33), administration of recombinant OPN to OPN-deficient mice reversed the ongoing remission of the disease and induced progressive exacerbation of the clinical symptoms (4). These findings prompted us to examine whether OPN is overexpressed in $CCR2^+$ $CCR5^+$ T cells after stimulation with PMA and ionomycin. As shown in Fig. 4D and 4E, $CCR2^+CCR5^+$ T cells expressed a much higher level of OPN than did the other memory T cell populations at both the mRNA and the protein levels.

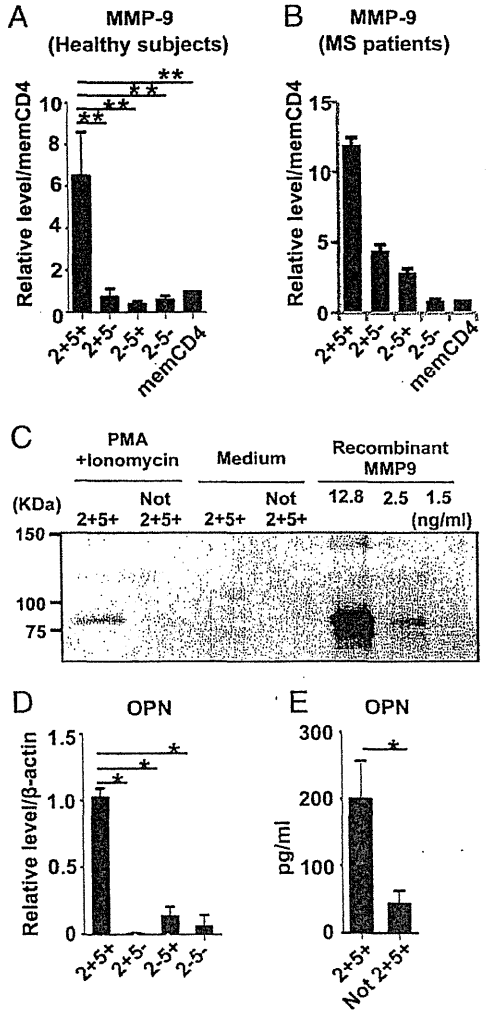

FIGURE 4. CCR2+CCR5+ T cells in the PB have the potential to produce MMP-9 and OPN. Each memory CD4+ T cell subset was isolated from the PBMC of HS (**A**) or MS (**B**) and was stimulated with PMA and ionomycin. Expression levels of MMP-9 mRNA were determined by quantitative RT-PCR. Results were normalized based on the values in unfractionated memory CD4+ T cells. Data represent mean ± SD of four HS or three MS patients. (**C**) CCR2+CCR5+ T cells and CD4+ T cells depleted of CCR2+CCR5+ T cells from HS were stimulated with PMA and ionomycin, and 20 μl of the culture supernatant and recombinant MMP-9 were electrophoresed. Shown are CCR2+CCR5+ T cells activated with PMA and ionomycin (*lane 1*), memory CD4+ T cells depleted of CCR2+ CCR5+ T cells activated with PMA and ionomycin (*lane 2*), CCR2+CCR5+ T cells without activation (*lane 3*), memory CD4+ T cells depleted of CCR2+CCR5+ T cells without activation (*lane 4*), and serial dilution of recombinant MMP-9 (*lanes 5–7*). The results shown are representative of three independent experiments. (**D**) Purified memory CD4+ T cell subsets from HS were stimulated with PMA and ionomycin. Expression levels of OPN mRNA were determined by quantitative RT-PCR. Data were normalized to the amount of β-actin mRNA. Data represent mean ± SD of four independent experiments. (**E**) Purified memory CD4+ T cell subsets were stimulated with PMA and ionomycin. OPN concentrations in the supernatants were measured by ELISA. Data represent mean ± SD of four different HS. $*p < 0.05$, $**p < 0.005$.

CCR2+CCR5+ T cells are superior to other T cells in the ability to invade the CNS

Although activated T cells are able to cross the endothelial barrier and enter the CSF compartment relatively easily, the parenchymal basement membrane and the glia limitans would hamper the further entry of the T cells into the CNS parenchyma. Although the endothelial cell basement membrane contains laminin-8 and -10, the parenchymal basal lamina is composed of laminin-1 or -2 (35). It was suggested that leukocyte penetration through the glia limitans requires MMP, such as MMP-2 and MMP-9 (36). After demonstrating that CCR2+CCR5+ T cells have the potential to produce MMP-9, we explored whether CCR2+CCR5+ T cells efficiently invade the CNS parenchyma across the basal lamina and glia limitans. To recapitulate the glia limitans layered with parenchymal basal lamina experimentally, we coated the upper sides of Transwell membrane inserts with laminin-1 or -2 and seeded NHA on the lower sides of the membrane inserts, as described in *Materials and Methods*. When we applied activated T cells to the upper chamber, their migration across the NHA layered with laminin-1 or -2 was less efficient compared with the migration across the untreated membrane or the membrane treated with laminin alone, as assessed by the number of migrated activated T cells collected from the lower chamber (Fig. 5A). Therefore, we assumed that this model would exhibit barrier functions against the penetration of activated T cells. Moreover, we applied CCR2+ CCR5+ T cells and memory CD4+ T cells depleted of CCR2+ CCR5+ T cells and showed that CCR2+CCR5+ T cells more efficiently penetrated and migrated to the lower chamber compared with the other T cells (Fig. 5B). These results indicate that CCR2+ CCR5+ T cells capable of producing MMP-9 and OPN have a greater potential to invade the brain parenchyma.

Table III. Primers used in this study

Primer	5′–3′
MMP1 forward	GATGAAGCAGCCCAGATGTGG
MMP1 reverse	GGAGAGTTGTCCCGATGATC
MMP9 forward	AGCGAGGTGGACCGGATGTTCC
MMP9 reverse	GAGCCCTAGTCCTCAGGGCA
MMP10 forward	GTGTGGAGTTCCTGACGTTGG
MMP10 reverse	GCATCTCTTGGCAAATCTGG
MMP19 forward	CAAGATGTCTCCTGGCTTCC
MMP19 reverse	CGGAGCCCTTAAAGAGGAACAC
MMP28 forward	TGCAGCTGCTACTGTGGGGCCA
MMP28 reverse	TCCAACACGCCGCTGACAGGTAGC
OPN forward	GGCAACGGGGATGGCCTTGT
OPN reverse	TTTTCCACGGACCTGCCAGCAAC
β-actin forward	CACTCTTCCAGCCTTCCTTCC
β-actin reverse	GCGTACAGGTCTTTGCGGATG
IFN-γ forward	CAGGTCATTCAGATGTAGCG
IFN-γ reverse	GCTTTTCGAAGTCATCTCG
IL-17 forward	CCAGGATGCCCAAATTCTGAGGAC
IL-17 reverse	CAAGGTGAGGTGGATCGGTTGTAG
RORC forward	AGAAGGACAGGGAGCCAAGG
RORC reverse	GTGATAACCCCGTAGTGGATC
T-bet forward	TCAGGGAAAGGACTCACCTG
T-bet reverse	AATAGCCTCCCCCATTCAAA

CCR2+CCR5+CCR6− subset producing IFN-γ and MMP-9 is selectively enriched in the CSF in MS

We noticed that CCR2+CCR5+ T cells consist of CCR6+ and CCR6− subset (Supplemental Fig. 1). Because Th17 cells appear to be enriched in CCR6+ T cells, we were interested to know whether CCR2+CCR5+ T cells could be functionally divided based on the expression of CCR6. When we compared the frequency of CCR2+CCR5+CCR6+ and CCR2+CCR5+CCR6− T cells between PB and CSF, the frequency of CCR6− subset was much higher in the CSF of MS in relapse than in PB ($p < 0.0005$), whereas the CCR6+ subset was not (Fig. 6A). Further analyses revealed that expression levels of IFN-γ in the CCR6− subset were higher than those in the CCR6+ subset, as assessed by RT-PCR (Fig. 6B). In contrast, the CCR6+ subset expressed much

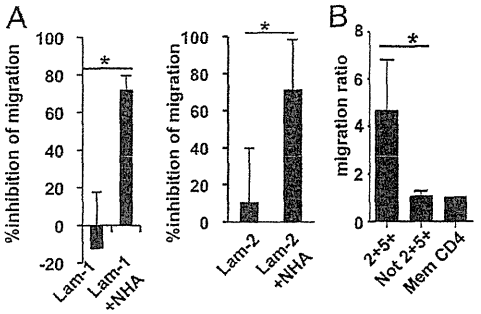

FIGURE 5. T cell migration across an in vitro glia limitans model. (**A**) The upper sides of Transwell membrane inserts were coated with laminin-1 (Lam-1; *left panel*) or laminin-2 (Lam-2; *right panel*), and NHA were seeded on the lower sides of the membrane inserts, as described in *Materials and Methods*. Unfractionated T cells isolated from PBMC were stimulated with PMA and ionomycin for 18 h and seeded onto the upper chambers. Eight hours later, absolute numbers of migrated cells were counted by flow cytometry. Data shown are the percentage inhibition of the migration, calculated as follows: [(migrated cell number through uncoated membrane) − (migrated cell number through membrane coated with laminin alone or laminin and NHA)] × 100/(migrated cell number through uncoated membrane). Data represent mean ± SD of four independent experiments. (**B**) PBMC from HS were sorted into memory $CD4^+CCR2^+CCR5^+$ T cells (2+5+), memory $CD4^+$ T cells depleted of $CCR2^+CCR5^+$ T cells (Not 2+5+), and unfractionated memory $CD4^+$ T cells (Mem CD4) by flow cytometry. The cells were stimulated with plate-bound anti-CD3/CD28 mAb for 60 h and seeded onto the upper chambers, whose membranes were coated with laminin-2 and NHA, as described in (A). Eight hours later, absolute numbers of migrated cells were counted by flow cytometry. To normalize individual variance, data are expressed as migration ratio of the number of migrated cells/number of migrated unfractionated memory $CD4^+$ T cells. Data represent mean ± SD of four independent experiments. $*p < 0.05$.

higher levels of IL-17 and RORC compared with the $CCR6^-$ subset. We also measured expression levels of MMP-9 mRNA; a much higher level of MMP-9 mRNA was found in the $CCR6^-$ subset (individual relative expression level from two samples = 1.0257 and 0.1127306) compared with the $CCR6^+$ subset (individual relative expression level = 0.0185 and 0.00345). Taken together, we postulate that $CCR2^+CCR5^+CCR6^-$ T cells producing IFN-γ, but not $CCR2^+CCR5^+CCR6^+$ T cells, play a crucial role in triggering the relapse of MS and expand in the CSF during relapse.

Discussion

Chemokines are a family of small chemotactic cytokines, which is a key to understanding the immune homeostasis, self-defense, and inflammation. Interactions between chemokines and their receptors are crucial for the migration of lymphocyte populations, such as T cells, macrophages, dendritic cells, and neutrophils, in autoimmune diseases, allergy, and cancer (37). Although chemokine receptor expression by the CSF lymphocytes or by brain-infiltrating T cells has been repeatedly investigated with regard to the pathogenesis of MS (38), most of the previous studies did not analyze the proportional changes of T cells simultaneously expressing more than two chemokine receptors. We showed that memory $CD4^+$ T cells expressing both CCR2 and CCR5 are selectively enriched in the CSF in MS during relapse but not in NIND or OIND.

Both CCR2 and CCR5 belong to the CC family of chemokines, which have two adjacent cysteines close to their N terminus. CCR2 binds CCL2 (MCP-1), CCL7 (MCP-3), CCL11 (eotaxin), CCL13 (MCP-4), and CCL16 (LEC), whereas CCR5 binds CCL3 (MIP-1α), CCL4 (MIP-1β), CCL5 (RANTES), CCL8, CCL11, CCL13, and CCL14. Among these chemokines, CCL5 was increased in the CSF in MS during acute relapses (39), and overexpression of CCL3 was detected in the brain tissues from MS (40). In contrast, CCL2 was decreased in the CSF in MS during relapses (38, 41), and this could be the result of consumption by $CCR2^+$ cells (42). Moreover, the presence of CCL2 and CCL5 was recently demonstrated in endothelial cells in brain samples from MS (43). CCL2 and CCL5 appear to play a critical role in adhesions of the encephalitogenic T cells to brain endothelial cells in a model of EAE (44). More recently, CCL2–CCR2 pairs were shown to play a critical role in the transendothelial migration of effector $CD4^+$ T cells (45), suggesting the importance of CCR2 expression for BBB transmigration. Taking these into consideration, we postulate that the chemokine gradient would facilitate the adherence of $CCR2^+CCR5^+$ T cells to the endothelial cells, as well as T cell entry into the CNS parenchyma during relapses of MS. Interestingly, $CCR2^-CCR5^+$ T cells, which produce a large quantity of IFN-γ, were also enriched in the CSF in MS. However, it was not specific for MS but was also present in the patients with NIND (Fig. 1C), indicating that only $CCR2^+CCR5^+$ T cells are specifically involved in the autoimmune pathology of MS. We subsequently found that the $CCR2^+CCR5^+$ T cells have an exceptional ability to produce MMP-9, an enzyme that is capable of disrupting the glia limitans, which led us to speculate that they have the

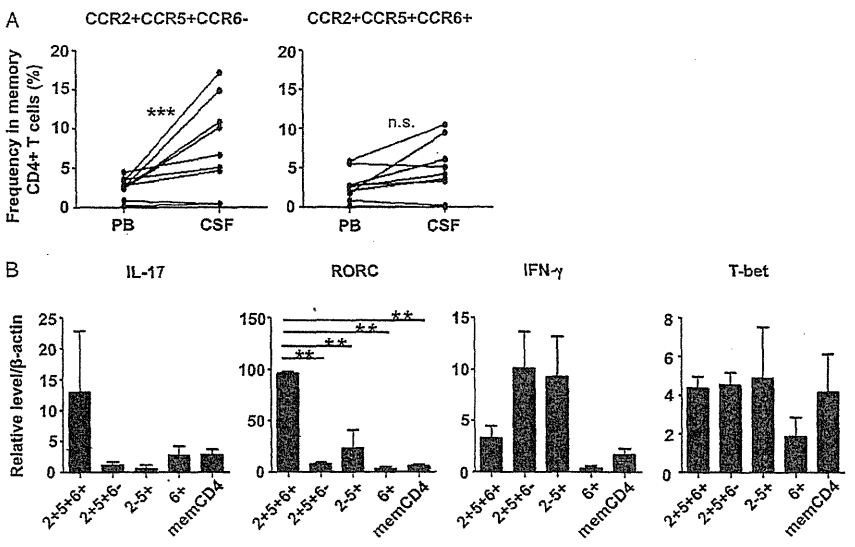

FIGURE 6. $CCR2^+CCR5^+CCR6^-$ T cells, but not $CCR2^+CCR5^+CCR6^+$ T cells, were enriched in the CSF of MS in relapse. (**A**) Cells were stained, as described in Fig. 1C, and frequencies of $CCR2^+CCR5^+CCR6^-$ and $CCR2^+CCR5^+CCR6^-$ T cells in the CSF and PB from nine MS patients in relapse were examined. Lines connect data from paired CSF and PB samples from the same patients. (**B**) Each memory $CD4^+$ T cell subset was isolated from the PBMC of HS and stimulated with PMA and ionomycin for 18 h. Expression levels of IL-17, IFN-γ, RORC, and T-bet mRNA were determined by quantitative RT-PCR. Data represent mean ± SD of three independent experiments. $**p < 0.005$, $***p < 0.0005$. n.s., Not significant.

potential to destroy the integrity of the BBB and trigger the cascade of inflammatory pathology. The MMP-9–producing CCR2+ CCR5+ T cells were indeed superior to the other T cells in their ability to cross the in vitro model of glia limitans layered by laminin-1 or -2.

MMP-9 appears to play a major role in EAE by disrupting the glia limitans, and a specific substrate of MMP-9 was shown to be dystroglycan, anchoring astrocyte end feet to parenchymal basement membrane via interaction with laminin-1 and -2 (36). Laminin-1 and -2 constitute the major laminin isoforms present in the CNS parenchymal basal lamina (35). Taken together, we postulate that the distinguished ability to produce MMP-9 would license the CCR2+CCR5+ T cells to serve as early invaders into the CNS parenchyma during relapses of MS. The CCR2+CCR5+ T cells also produce a large amount of OPN, an integrin-binding protein abundantly expressed in active MS lesions (33). OPN is a pleiotropic protein that interacts with various integrins. In addition to its function as an adhesion molecule, OPN promotes the survival of activated T cells and the production of proinflammatory cytokines by APC (46). It is very likely that paracrine OPN produced by the CCR2+CCR5+ T cells would promote the survival of these MMP-9–producing T cells in the CNS, which leads to further enrichment of the CCR2+CCR5+ T cells in the CSF.

Seeing the specific increase in the CCR2+CCR5+ T cells in the CSF in MS, we were very curious to know whether this T cell population is enriched with autoimmune T cells critical for the initiation of MS pathology. By stimulating the PB CCR2+CCR5+ T cells with MBP, we showed that, in patients with MS relapse, this T cell subset produces a large quantity of IFN-γ and some IL-17 in response to MBP, a representative autoantigen for MS (Fig. 3C). In contrast, the cells from MS in remission or from healthy controls did not respond significantly. Although we did not examine the CSF T cells' response to MBP because of a technical difficulty, it is likely that the CCR2+CCR5+ T cells in the CSF in MS during relapse are enriched with MBP-reactive autoimmune T cells as well.

Of note, Zhang et al. (47) recently reported that CCR2+CCR5+ cells are highly differentiated, yet stable, effector memory CD4+ T cells equipped for provoking rapid recall response. They showed evidence that CCR2+CCR5+ T cells should have undergone reactivation and subsequent proliferation more often than other memory T cell subsets and are resistant to apoptosis. Thus, it is likely that autoreactive T cells are enriched in CCR2+CCR5+ T cells that have survived following repeated reactivation over a long period of time. We assume that once autoreactive T cells differentiate into stable effector memory T cells expressing CCR2 and CCR5, they might persist and trigger relapse repeatedly. We further revealed that the CCR6−, but not the CCR6+, subset of CCR2+CCR5+ T cells was significantly enriched in the CSF of MS patients during relapse.

Reboldi et al. (48) reported that CCR6+ T cells are more enriched in CSF than in the PB of clinically isolated syndrome (CIS). Diagnosis of CIS can be made when patients developed a single attack of neurologic disability that is consistent with demyelinating pathology and that may turn out to be the first episode of MS (49). However, in our Japanese patients having clinically definite MS, we did not detect enrichment of CCR6+ T cells in the CSF. Rather, T cells bearing Th17 phenotypes appeared to be prohibited from entry into the CNS in MS. The difference between the results in CIS and MS could be explained by the premise that autoimmune pathology may be premature at the CIS stage. In contrast, the increase in CCR2+CCR5+ T cells in the CSF was not detected in the patients who had MS for >10 y. These observations are in accordance with the postulate that acquired and innate immune components, as well as neurodegenerative components, differentially contribute to the different stages of MS (50).

In summary, we identified a unique CCR2+CCR5+CCR6− T cell population that is enriched in the CSF of patients with exacerbated MS. Our data suggest that targeting this population may be a novel therapeutic approach for MS.

Acknowledgments

We thank Dr. Britta Engelhardt for valuable comments and Hiromi Yamaguchi and Ryoko Saga for excellent technical assistance.

Disclosures

The authors have no financial conflicts of interest.

References

1. McFarland, H. F., and R. Martin. 2007. Multiple sclerosis: a complicated picture of autoimmunity. *Nat. Immunol.* 8: 913–919.
2. Trapp, B. D., and K. A. Nave. 2008. Multiple sclerosis: an immune or neurodegenerative disorder? *Annu. Rev. Neurosci.* 31: 247–269.
3. Wucherpfennig, K. W., and J. L. Strominger. 1995. Molecular mimicry in T cell-mediated autoimmunity: viral peptides activate human T cell clones specific for myelin basic protein. *Cell* 80: 695–705.
4. Hur, E. M., S. Youssef, M. E. Haws, S. Y. Zhang, R. A. Sobel, and L. Steinman. 2007. Osteopontin-induced relapse and progression of autoimmune brain disease through enhanced survival of activated T cells. *Nat. Immunol.* 8: 74–83.
5. Ransohoff, R. M., P. Kivisäkk, and G. Kidd. 2003. Three or more routes for leukocyte migration into the central nervous system. *Nat. Rev. Immunol.* 3: 569–581.
6. Bartholomäus, I., N. Kawakami, F. Odoardi, C. Schläger, D. Miljkovic, J. W. Ellwart, W. E. Klinkert, C. Flügel-Koch, T. B. Issekutz, H. Wekerle, and A. Flügel. 2009. Effector T cell interactions with meningeal vascular structures in nascent autoimmune CNS lesions. *Nature* 462: 94–98.
7. Gijbels, K., R. E. Galardy, and L. Steinman. 1994. Reversal of experimental autoimmune encephalomyelitis with a hydroxamate inhibitor of matrix metalloproteases. *J. Clin. Invest.* 94: 2177–2182.
8. Engelhardt, B. 2010. T cell migration into the central nervous system during health and disease: Different molecular keys allow access to different central nervous system compartments. *Clin. Exp. Neuroimmunol.* 1: 79–93.
9. Steinman, L. 2009. Shifting therapeutic attention in MS to osteopontin, type 1 and type 2 IFN. *Eur. J. Immunol.* 39: 2358–2360.
10. Aranami, T., and T. Yamamura. 2008. Th17 Cells and autoimmune encephalomyelitis (EAE/MS). *Allergol. Int.* 57: 115–120.
11. Tzartos, J. S., M. A. Friese, M. J. Craner, J. Palace, J. Newcombe, M. M. Esiri, and L. Fugger. 2008. Interleukin-17 production in central nervous system-infiltrating T cells and glial cells is associated with active disease in multiple sclerosis. *Am. J. Pathol.* 172: 146–155.
12. Kebir, H., I. Ifergan, J. I. Alvarez, M. Bernard, J. Poirier, N. Arbour, P. Duquette, and A. Prat. 2009. Preferential recruitment of interferon-gamma-expressing TH17 cells in multiple sclerosis. *Ann. Neurol.* 66: 390–402.
13. Panitch, H. S., R. L. Hirsch, A. S. Haley, and K. P. Johnson. 1987. Exacerbations of multiple sclerosis in patients treated with gamma interferon. *Lancet* 1: 893–895.
14. Broux, B., K. Pannemans, X. Zhang, S. Markovic-Plese, T. Broekmans, B. O. Eijnde, B. Van Wijmeersch, V. Somers, P. Geusens, S. van der Pol, et al. 2012. CX(3)CR1 drives cytotoxic CD4(+)CD28(−) T cells into the brain of multiple sclerosis patients. *J. Autoimmun.* 38: 10–19.
15. Saxena, A., G. Martin-Blondel, L. T. Mars, and R. S. Liblau. 2011. Role of CD8 T cell subsets in the pathogenesis of multiple sclerosis. *FEBS Lett.* 585: 3758–3763.
16. Segal, B. M., C. S. Constantinescu, A. Raychaudhuri, L. Kim, R. Fidelus-Gort, and L. H. Kasper; Ustekinumab MS Investigators. 2008. Repeated subcutaneous injections of IL12/23 p40 neutralising antibody, ustekinumab, in patients with relapsing-remitting multiple sclerosis: a phase II, double-blind, placebo-controlled, randomised, dose-ranging study. *Lancet Neurol.* 7: 796–804.
17. Mackay, C. R. 2001. Chemokines: immunology's high impact factors. *Nat. Immunol.* 2: 95–101.
18. Proudfoot, A. E. 2002. Chemokine receptors: multifaceted therapeutic targets. *Nat. Rev. Immunol.* 2: 106–115.
19. Izikson, L., R. S. Klein, I. F. Charo, H. L. Weiner, and A. D. Luster. 2000. Resistance to experimental autoimmune encephalomyelitis in mice lacking the CC chemokine receptor (CCR)2. *J. Exp. Med.* 192: 1075–1080.
20. Sallusto, F., and A. Lanzavecchia. 2000. Understanding dendritic cell and T-lymphocyte traffic through the analysis of chemokine receptor expression. *Immunol. Rev.* 177: 134–140.
21. Nagata, K., K. Tanaka, K. Ogawa, K. Kemmotsu, T. Imai, O. Yoshie, H. Abe, K. Tada, M. Nakamura, K. Sugamura, and S. Takano. 1999. Selective expression

of a novel surface molecule by human Th2 cells in vivo. *J. Immunol.* 162: 1278–1286.
22. Ransohoff, R. M. 2009. Chemokines and chemokine receptors: standing at the crossroads of immunobiology and neurobiology. *Immunity* 31: 711–721.
23. Acosta-Rodriguez, E. V., L. Rivino, J. Geginat, D. Jarrossay, M. Gattorno, A. Lanzavecchia, F. Sallusto, and G. Napolitani. 2007. Surface phenotype and antigenic specificity of human interleukin 17-producing T helper memory cells. *Nat. Immunol.* 8: 639–646.
24. Sato, W., T. Aranami, and T. Yamamura. 2007. Cutting edge: Human Th17 cells are identified as bearing CCR2+CCR5− phenotype. *J. Immunol.* 178: 7525–7529.
25. Singh, S. P., H. H. Zhang, J. F. Foley, M. N. Hedrick, and J. M. Farber. 2008. Human T cells that are able to produce IL-17 express the chemokine receptor CCR6. *J. Immunol.* 180: 214–221.
26. McDonald, W. I., A. Compston, G. Edan, D. Goodkin, H. P. Hartung, F. D. Lublin, H. F. McFarland, D. W. Paty, C. H. Polman, S. C. Reingold, et al. 2001. Recommended diagnostic criteria for multiple sclerosis: guidelines from the International Panel on the diagnosis of multiple sclerosis. *Ann. Neurol.* 50: 121–127.
27. Takahashi, K., T. Aranami, M. Endoh, S. Miyake, and T. Yamamura. 2004. The regulatory role of natural killer cells in multiple sclerosis. *Brain* 127: 1917–1927.
28. Leppert, D., J. Ford, G. Stabler, C. Grygar, C. Lienert, S. Huber, K. M. Miller, S. L. Hauser, and L. Kappos. 1998. Matrix metalloproteinase-9 (gelatinase B) is selectively elevated in CSF during relapses and stable phases of multiple sclerosis. *Brain* 121: 2327–2334.
29. Sallusto, F., J. Geginat, and A. Lanzavecchia. 2004. Central memory and effector memory T cell subsets: function, generation, and maintenance. *Annu. Rev. Immunol.* 22: 745–763.
30. Toft-Hansen, H., R. Buist, X. J. Sun, A. Schellenberg, J. Peeling, and T. Owens. 2006. Metalloproteinases control brain inflammation induced by pertussis toxin in mice overexpressing the chemokine CCL2 in the central nervous system. *J. Immunol.* 177: 7242–7249.
31. Stüve, O., N. P. Dooley, J. H. Uhm, J. P. Antel, G. S. Francis, G. Williams, and V. W. Yong. 1996. Interferon beta-1b decreases the migration of T lymphocytes in vitro: effects on matrix metalloproteinase-9. *Ann. Neurol.* 40: 853–863.
32. Bar-Or, A., R. K. Nuttall, M. Duddy, A. Alter, H. J. Kim, I. Ifergan, C. J. Pennington, P. Bourgoin, D. R. Edwards, and V. W. Yong. 2003. Analyses of all matrix metalloproteinase members in leukocytes emphasize monocytes as major inflammatory mediators in multiple sclerosis. *Brain* 126: 2738–2749.
33. Chabas, D., S. E. Baranzini, D. Mitchell, C. C. Bernard, S. R. Rittling, D. T. Denhardt, R. A. Sobel, C. Lock, M. Karpuj, R. Pedotti, et al. 2001. The influence of the proinflammatory cytokine, osteopontin, on autoimmune demyelinating disease. *Science* 294: 1731–1735.
34. Shinohara, M. L., M. Jansson, E. S. Hwang, M. B. Werneck, L. H. Glimcher, and H. Cantor. 2005. T-bet-dependent expression of osteopontin contributes to T cell polarization. *Proc. Natl. Acad. Sci. USA* 102: 17101–17106.
35. Sixt, M., B. Engelhardt, F. Pausch, R. Hallmann, O. Wendler, and L. M. Sorokin. 2001. Endothelial cell laminin isoforms, laminins 8 and 10, play decisive roles in T cell recruitment across the blood-brain barrier in experimental autoimmune encephalomyelitis. *J. Cell Biol.* 153: 933–946.
36. Agrawal, S., P. Anderson, M. Durbeej, N. van Rooijen, F. Ivars, G. Opdenakker, and L. M. Sorokin. 2006. Dystroglycan is selectively cleaved at the parenchymal basement membrane at sites of leukocyte extravasation in experimental autoimmune encephalomyelitis. *J. Exp. Med.* 203: 1007–1019.
37. Moser, B., and P. Loetscher. 2001. Lymphocyte traffic control by chemokines. *Nat. Immunol.* 2: 123–128.
38. Sørensen, T. L., M. Tani, J. Jensen, V. Pierce, C. Lucchinetti, V. A. Folcik, S. Qin, J. Rottman, F. Sellebjerg, R. M. Strieter, et al. 1999. Expression of specific chemokines and chemokine receptors in the central nervous system of multiple sclerosis patients. *J. Clin. Invest.* 103: 807–815.
39. Kivisäkk, P., C. Trebst, Z. Liu, B. H. Tucky, T. L. Sørensen, R. A. Rudick, M. Mack, and R. M. Ransohoff. 2002. T-cells in the cerebrospinal fluid express a similar repertoire of inflammatory chemokine receptors in the absence or presence of CNS inflammation: implications for CNS trafficking. *Clin. Exp. Immunol.* 129: 510–518.
40. Balashov, K. E., J. B. Rottman, H. L. Weiner, and W. W. Hancock. 1999. CCR5(+) and CXCR3(+) T cells are increased in multiple sclerosis and their ligands MIP-1alpha and IP-10 are expressed in demyelinating brain lesions. *Proc. Natl. Acad. Sci. USA* 96: 6873–6878.
41. Franciotta, D., G. Martino, E. Zardini, R. Furlan, R. Bergamaschi, L. Andreoni, and V. Cosi. 2001. Serum and CSF levels of MCP-1 and IP-10 in multiple sclerosis patients with acute and stable disease and undergoing immunomodulatory therapies. *J. Neuroimmunol.* 115: 192–198.
42. Mahad, D., M. K. Callahan, K. A. Williams, E. E. Ubogu, P. Kivisäkk, B. Tucky, G. Kidd, G. A. Kingsbury, A. Chang, R. J. Fox, et al. 2006. Modulating CCR2 and CCL2 at the blood-brain barrier: relevance for multiple sclerosis pathogenesis. *Brain* 129: 212–223.
43. Subileau, E. A., P. Rezaie, H. A. Davies, F. M. Colyer, J. Greenwood, D. K. Male, and I. A. Romero. 2009. Expression of chemokines and their receptors by human brain endothelium: implications for multiple sclerosis. *J. Neuropathol. Exp. Neurol.* 68: 227–240.
44. dos Santos, A. C., M. M. Barsante, R. M. Arantes, C. C. Bernard, M. M. Teixeira, and J. Carvalho-Tavares. 2005. CCL2 and CCL5 mediate leukocyte adhesion in experimental autoimmune encephalomyelitis—an intravital microscopy study. *J. Neuroimmunol.* 162: 122–129.
45. Shulman, Z., S. J. Cohen, B. Roediger, V. Kalchenko, R. Jain, V. Grabovsky, E. Klein, V. Shinder, L. Stoler-Barak, S. W. Feigelson, et al. 2012. Transendothelial migration of lymphocytes mediated by intraendothelial vesicle stores rather than by extracellular chemokine depots. *Nat. Immunol.* 13: 67–76.
46. Denhardt, D. T., M. Noda, A. W. O'Regan, D. Pavlin, and J. S. Berman. 2001. Osteopontin as a means to cope with environmental insults: regulation of inflammation, tissue remodeling, and cell survival. *J. Clin. Invest.* 107: 1055–1061.
47. Zhang, H. H., K. Song, R. L. Rabin, B. J. Hill, S. P. Perfetto, M. Roederer, D. C. Douek, R. M. Siegel, and J. M. Farber. 2010. CCR2 identifies a stable population of human effector memory CD4+ T cells equipped for rapid recall response. *J. Immunol.* 185: 6646–6663.
48. Reboldi, A., C. Coisne, D. Baumjohann, F. Benvenuto, D. Bottinelli, S. Lira, A. Uccelli, A. Lanzavecchia, B. Engelhardt, and F. Sallusto. 2009. C-C chemokine receptor 6-regulated entry of TH-17 cells into the CNS through the choroid plexus is required for the initiation of EAE. *Nat. Immunol.* 10: 514–523.
49. Miller, D., F. Barkhof, X. Montalban, A. Thompson, and M. Filippi. 2005. Clinically isolated syndromes suggestive of multiple sclerosis, part I: natural history, pathogenesis, diagnosis, and prognosis. *Lancet Neurol.* 4: 281–288.
50. Weiner, H. L. 2008. A shift from adaptive to innate immunity: a potential mechanism of disease progression in multiple sclerosis. *J. Neurol.* 255(Suppl. 1): 3–11.

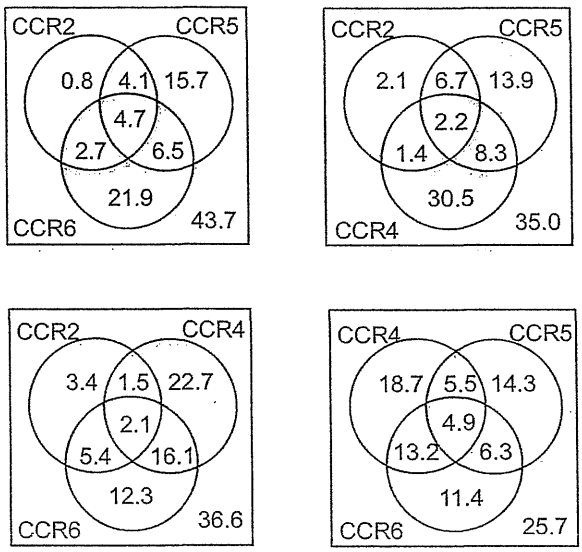

SUPPLEMENTAL FIGURE 1. Chemokine receptor expression profiles and its overlap in memory CD4$^+$ T cells from MS

For flow cytometric analysis, PBMC depleted of CD14$^+$ cells were stained with differentially labeled anti-CD4, -CD45RA, -CCR2, -CCR5, -CCR4 and -CCR6 mAbs simultaneously. Venn diagrams show frequencies (%) of the cells expressing CCR2, CCR4, CCR5 and CCR6 in memory CD4$^+$ T cells in PB from 11 MS patients in remission. The combination of 3 chemokine receptors out of 4 is shown in each panel.

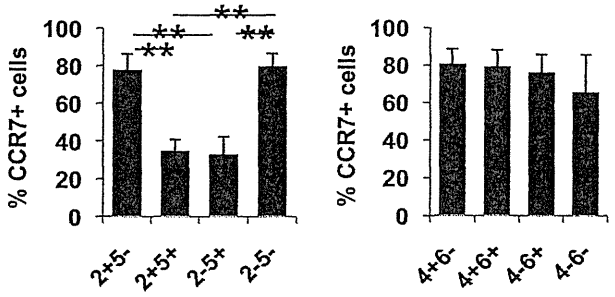

SUPPLEMENTAL FIGURE 2. Frequency of CCR7 expression in memory CD4$^+$ T cell subsets defined by chemokine receptor expression profile
Shown are the proportions of CCR7$^+$ cells within each memory CD4$^+$ T cell subset defined by expression of CCR2 and CCR5 (left), and of CCR4 and CCR6 (right).

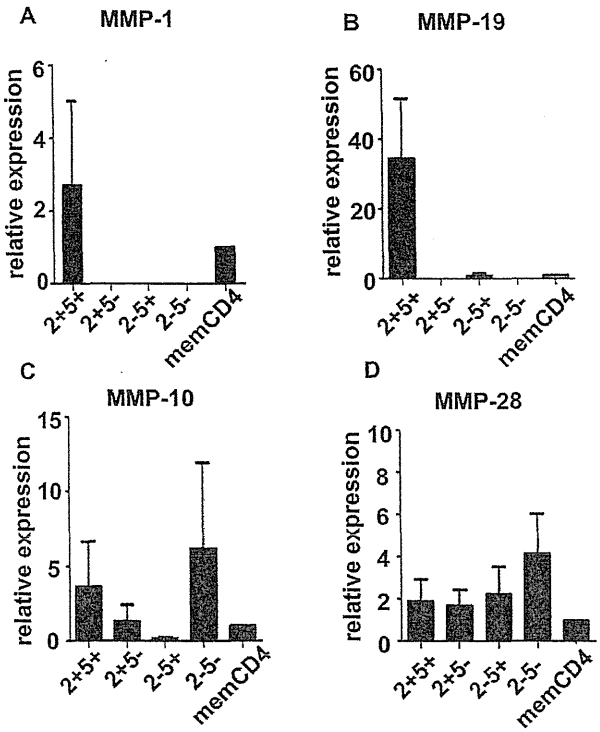

SUPPLEMENTAL FIGURE 3. Expression levels of MMP-1, -19, -10, and -28 in memory CD4$^+$ T cells
Each memory CD4$^+$ T cell subset was purified from the PB of HS individuals and was stimulated with PMA and ionomycin. The expression levels of the MMP mRNAs were determined by quantitative RT-PCR. Data represent mean values ± SD of 4 different subjects.

Supplemental Table. Frequencies of memory CD4$^+$ T cell subsets determined by chemokine receptor expression

	HS (%)	MS (%)
2+5+4+6−	0.69±0.46	1.05±0.59
2+5+4+6+	0.88±0.87	1.09±0.78
2+5+4−6+	2.91±2.47	3.6±1.72
2+5+4−6−	3.05±1.91	3.08±1.05
2+5−4+6−	0.27±0.24	0.4±0.37
2+5−4+6+	0.57±0.49	0.95±0.79
2+5−4−6+	1.35±1.35	1.78±1.21
2+5−4−6−	0.46±0.25	0.36±0.19
2−5+4+6−	3.49±1.52	4.43±1.82
2−5+4+6+	3.63±1.95	3.84±1.39
2−5+4−6+	2.19±0.92	2.67±1.22
2−5+4−6−	9.38±4.61	11.26±6.79
2−5−4+6−	18.72±5.07	18.32±5.01
2−5−4+6+	11.91±3.91	12.21±3.34
2−5−4−6+	9.04±3.10	9.62±1.53
2−5−4−6−	31.49±8.55	25.33±4.83

Memory CD4+ T cells were divided into 16 subsets based on the expression of CCR2, CCR5, CCR4, and CCR6. Data from 11 HS and 11 patients with MS in remission were analyzed.

INTERNAL MEDICINE

CASE REPORT

New-Onset Type 1 Diabetes Mellitus and Anti-Aquaporin-4 Antibody Positive Optic Neuritis Associated with Type 1 Interferon Therapy for Chronic Hepatitis C

Tomoya Kawazoe[1], Manabu Araki[1], Youwei Lin[1], Masafumi Ogawa[1], Tomoko Okamoto[1], Takashi Yamamura[2], Masato Wakakura[3] and Miho Murata[1]

Abstract

A 60-year-old woman developed type 1 diabetes mellitus and anti-aquaporin-4 antibody positive optic neuritis during type 1 interferon therapies for chronic hepatitis C. The diabetes mellitus was elicited by interferon-α plus ribavirin therapy, while the optic neuritis was induced after interferon-β treatment, followed by interferon-α and ribavirin therapy. It is possible that type 1 interferons lead to the onset of the two autoimmune diseases by inducing disease-specific autoantibodies. Autoimmune disease is an infrequent complication of type 1 interferon treatment; however, once it has occurred, it may result in severe impairments. Patients undergoing type 1 interferon therapy should therefore be carefully monitored for any manifestations of autoimmune diseases.

Key words: aquaporin-4, neuromyelitis optica, chronic hepatitis C, type 1 diabetes mellitus, type 1 interferon

(Intern Med 51: 2625-2629, 2012)
(DOI: 10.2169/internalmedicine.51.7771)

Introduction

Type 1 interferon (IFN) is widely used to treat patients with chronic viral hepatitis and malignant neoplasms. Approximately two million people in Japan are infected with the hepatitis C virus (HCV). Combination therapy with type 1 IFN and ribavirin (RBV) is used in 50,000-100,000 patients annually. Since type 1 IFN has not only antiviral and antiproliferative effects, but also immunomodulatory effects, it can occasionally induce various autoimmune diseases (1). The onset of autoimmune diseases can be attributed to the overproduction of disease-specific antibodies. We herein present the case of a patient who developed type 1 diabetes mellitus (T1DM) and severe optic neuritis with anti-aquaporin-4 (AQP-4) antibodies during treatment with combinations including IFN-α and IFN-β for chronic hepatitis C.

Case Report

A 60-year-old Japanese woman was diagnosed with hepatitis C (type 1b) in 1994 at the age of 42 years. Since the diagnosis, she had received various types of IFN therapy: natural IFN-α, recombinant IFN-α-2b and RBV, recombinant IFN-αcon-1, and pegylated IFN (PEG-IFN)-α-2b and RBV (Fig. 1). From 1994 to 2008, all of the above-mentioned IFN therapies resulted in a transient reduction in HCV-RNA to undetectable levels, but a sustained virologic response (SVR) was not obtained. While undergoing PEG-IFN/RBV treatment, the patient was noted to have hyperglycemia, and she was diagnosed with T1DM in 2008 (Fig. 1). She was found to be positive for anti-glutamic acid decarboxylase (GAD) antibodies, with a titer of 3,440x. The titers of anti-GAD antibodies were decreased to 128x two years after the initiation of insulin treatment.

In January 2009, the patient underwent combination therapy for virus eradication by double-filtration plasmapheresis

[1]Department of Neurology, National Center Hospital, National Center of Neurology and Psychiatry, Japan, [2]Department of Immunology, National Institute of Neuroscience, National Center of Neurology and Psychiatry, Japan and [3]Inouye Eye Hospital, Japan
Received for publication May 24, 2012; Accepted for publication June 25, 2012
Correspondence to Dr. Manabu Araki, m-araki@ncnp.go.jp

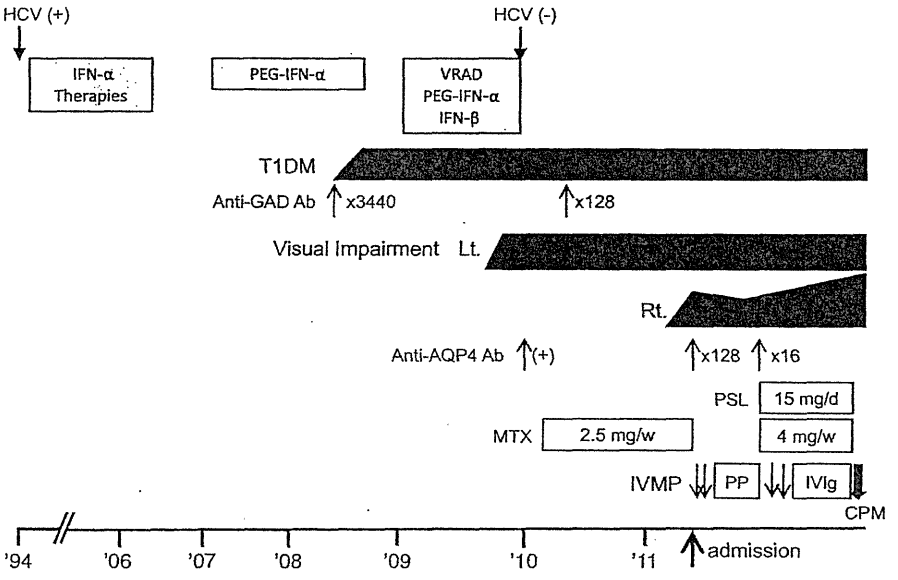

Figure 1. The clinical course of the present case. Anti-AQP-4 Ab: anti-aquaporin-4 antibody, Anti-GAD antibody: Anti-glutamic acid decarboxylase antibody, CPM: cyclophosphamide, HCV: hepatitis C virus, IFN-a therapies: IFN-α for 24 weeks from 1994 to 1995, IFN-α-2b/Ribavirin (RBV) for 24 weeks in 2002, IFN-αcon-1 for 12 weeks in 2004, and PEG-IFN-α-2b/RBV for 48 weeks from 2005 to 2006, IVIg: intravenous immunoglobulin, IVMP: intravenous methylprednisolone, MTX: methotrexate, PEG-IFN: pegylated IFN-α-2b and RBV, PP: plasmapheresis, PSL: prednisolone, T1DM: type 1 diabetes mellitus, VRAD: virus removal and eradication by double-filtration plasmapheresis (DFPP)

(VRAD), intravenous natural IFN-β for 14 days, and PEG-IFN-α-2a plus RBV for 36 weeks to achieve HCV-RNA seronegativity. A SVR was finally achieved with these intensive combination therapies (Fig. 1).

In November 2009, the patient experienced pain when moving her left eye. Her left visual acuity deteriorated to light perception within two weeks. She was diagnosed with left optic neuritis. The IFN therapy was terminated, and triamcinolone was injected locally into the subtenon of the affected side, which was not effective. Serological tests demonstrated that she was positive for AQP-4 antibodies in January 2010, and hence a clinical diagnosis of neuromyelitis optica spectrum disorder (NMOsd) was made (Fig. 1).

To prevent relapse and progression of the optic neuritis, immunosuppressant drug therapy was initiated, with weekly oral methotrexate (MTX) administration at a dose of 2.5 mg. In June 2011, right optic neuritis occurred and the right visual acuity was decreased from normal to finger counting within two weeks. She received two courses of high-dose intravenous methylprednisolone (IVMP) therapy, which were not effective. She was admitted to our hospital for further treatment (Fig. 1).

On admission, her neurological findings were normal, except for the severe visual impairment of 0.02 (20/1,000) in both eyes. The visual field defects were detected by Goldmann perimetry (Fig. 2A). Ophthalmoscopy showed no impairment of the retinal blood vessels. The visual evoked potential indicated no response. The cerebrospinal fluid was normal, with a cell count of less than 1/μL with all mononuclear cells, and a protein concentration of 37 mg/dL. Oligoclonal banding was negative, and the myelin basic protein level was within the normal range. The serum blood sugar level was 196 mg/dL (normal range 70-110), glycosylated hemoglobin was 6.7% (normal range 4.3-5.8), and the anti-GAD antibodies were detected with a value of 9.9 U/mL. The patient's serum was also found to be positive for anti-AQP-4 antibodies, with a titer of 128x. Anti-nuclear antibodies, anti-SS-A/SS-B antibodies, anti-neutrophil cytoplasmic antibodies, and anti-thyroid antibodies were not detected.

Magnetic resonance imaging (MRI) showed a high signal intensity of the left optic nerve on T2-weighted and fluid-attenuated inversion recovery, and T1-weighted imaging with contrast enhancement, whereas the right optic nerve showed no particular findings (Fig. 2B, C). Brain MRI (Fig. 2D, E) showed a small number of high-intensity spots in the cerebral white matter. No obvious abnormality was observed in the spinal cord MRI.

The patient was treated with eight courses of plasmapheresis. During the treatment, her visual acuity slightly improved and she could read a few written characters. The titer of the anti-AQP-4 antibodies was decreased to 16x. However, the patient's visual field defect gradually worsened again soon after the discontinuation of plasmapheresis, so we initiated two courses of IVMP therapy, an additional two courses of plasmapheresis, high-dose intravenous immu-